



SPECIAL FEATURE: VEGETATION SURVEY

Vegetation of zonal patterned-ground ecosystems along the North America Arctic bioclimate gradient

Donald A. Walker, Patrick Kuss, Howard E. Epstein, Anja N. Kade, Corinne M. Vonlanthen, Martha K. Raynolds & Fred J.A. Daniëls

Keywords

Biocomplexity; Biomass; Climate gradient; Frost heave; JUICE; *n*-factor; Non-metric multidimensional scaling (NMDS); Normalized difference vegetation index (NDVI);.

Abbreviations

AK = Alaska; CAN = Canada; MAT = Moist acidic tundra; MNT = Moist non-acidic tundra; NAAT = North American Arctic Transect; PGF = patterned-ground feature; bPGF = between patterned-ground features; iPGF = intermediate position in patterned-ground features; SWI = summer warmth index; NDVI = Normalized difference vegetation index.

Nomenclature:

Elven et al. 2007 (vascular plants); Ignatov & Afonina 1992 (mosses); Konstantinova et al. 1992 (liverworts); Esslinger 2008, Kristinsson et al. 2010 (lichens).

Received 21 October 2010

Accepted 1 June 2011

Co-ordinating Editor: Angelika Schwabe-Kratochwil

Walker, D.A. (corresponding author, dawalker@alaska.edu): Alaska Geobotany Center, Institute of Arctic Biology, University of Alaska Fairbanks, 311 Irving, P.O. Box 757000, Fairbanks, AK 99775, USA

Kuss, P. (patrick.kuss@ips.unibe.ch): Institute of Plant Sciences, University of Bern, Altenbergrain 21, 3013 Bern, Switzerland

Epstein, H.E. (hee2b@virginia.edu): Department of Environmental Sciences, University of Virginia 22904, USA

Kade, A.N. (anja_kade@yahoo.com): Institute of Arctic Biology, University of Alaska Fairbanks, 311 Irving, P.O. Box 757000, Fairbanks, AK 99775, USA

Vonlanthen, C.M. (corinne.vonlanthen@bafu.admin.ch): Bundesamt für Umwelt BAFU, Abteilung Gefahrenprävention, 3003 Bern, Switzerland

Raynolds, M.K. (mraynolds@alaska.edu): Alaska Geobotany Center, Institute of Arctic

Abstract

Question: How do interactions between the physical environment and biotic properties of vegetation influence the formation of small patterned-ground features along the Arctic bioclimate gradient?

Location: At 68° to 78°N: six locations along the Dalton Highway in arctic Alaska and three in Canada (Banks Island, Prince Patrick Island and Ellef Ringnes Island).

Methods: We analysed floristic and structural vegetation, biomass and abiotic data (soil chemical and physical parameters, the *n*-factor [a soil thermal index] and spectral information [NDVI, LAI]) on 147 microhabitat relevés of zonal-patterned-ground features. Using mapping, table analysis (JUICE) and ordination techniques (NMDS).

Results: Table analysis using JUICE and the phi-coefficient to identify diagnostic species revealed clear groups of diagnostic plant taxa in four of the five zonal vegetation complexes. Plant communities and zonal complexes were generally well separated in the NMDS ordination. The Alaska and Canada communities were spatially separated in the ordination because of different glacial histories and location in separate floristic provinces, but there was no single controlling environmental gradient. Vegetation structure, particularly that of bryophytes and total biomass, strongly affected thermal properties of the soils. Patterned-ground complexes with the largest thermal differential between the patterned-ground features and the surrounding vegetation exhibited the clearest patterned-ground morphologies.

Conclusions: Characterizing the composition and structure of small-scale plant communities growing on distinctive microhabitats within patterned-ground complexes was necessary to understand the biological and physical controls of vegetation on patterned-ground morphology. Coarser-scale vegetation units, referred to here as 'zonal patterned-ground vegetation complexes' (groups of patterned-ground plant communities within zonal landscapes), were useful for landscape and regional-level comparisons and for extrapolation of information collected at plot scales to larger regions. Vegetation maps of the representative landscapes in each subzone were needed for extrapolation. Different growth characteristics of plants growing in northern and southern parts of the gradient have an important effect in stabilizing highly frost-active soils. A conceptual diagram summarizes the interactions between vegetation and patterned-ground morphology along the Arctic climate gradient.

Biology, University of Alaska Fairbanks, 311 Irving, P.O. Box 757000, Fairbanks, AK 99775, USA

Daniëls, F.J.A. (daniels@uni-muenster.de): Institute of Biology and Biotechnology of Plants, Hindenburgplatz 55, 48143, Münster, Germany.

Introduction

Arctic landscapes that are underlain by permafrost typically have small patterned-ground landforms that are a few centimeters to 1–3 m in diameter that include small and medium-size non-sorted polygons, non-sorted circles (frost boils) and earth hummocks (Fig. 1). Table 1 presents the patterned-ground classification system used for describing small patterned-ground features (PGFs). These features have interested geologists and geographers for decades (Hopkins & Sigafos 1951; Nicholson 1976;

Washburn 1980; Hallet 1987; Kessler & Werner 2003). More recently, there has been renewed interest in these features because of their possible importance in a wide range of tundra ecosystem properties and processes, including tundra carbon, water and nutrient dynamics and the effect that these features have on the spectral properties of regional tundra ecosystems (Matveyeva 1998; Walker et al. 2004a,b, 2008a; Shur et al. 2005, 2008; Kokelj et al. 2007; Epstein et al. 2008). Common hypotheses for the formation of these small patterned-ground features (PGFs) include desiccation cracking,

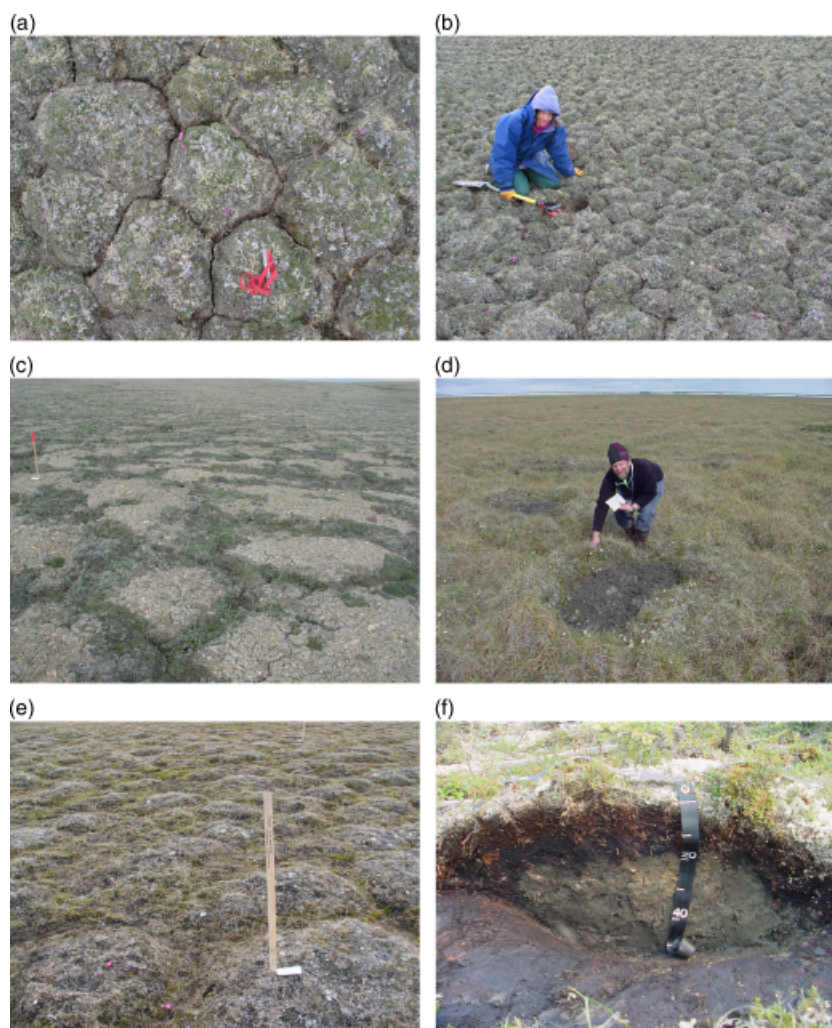


Fig. 1. Small patterned-ground features. **(a, b)** Small non-sorted polygons about 10–20-cm diameter at Green Cabin, Banks Island, Canada (bioclimate subzone C) that have become rounded and well vegetated with *Dryas integrifolia* a few forbs and lichens. **(c)** Non-sorted circles formed in the centre of medium-size, non-sorted polygons, Green Cabin, Banks Island, Canada (bioclimate subzone C); diameter of barren surfaces is 80–120 cm. **(d)** Non-sorted circle in well-vegetated tundra, Franklin Bluffs, AK, (bioclimate subzone D); diameter of circle is about 70 cm. **(e)** Earth hummocks, Mould Bay, Prince Patrick Island, Canada (bioclimate subzone B). Diameters are about 80–100 cm. **(f)** View of interior of earth hummock near Inuvik, NWT, Canada. Dark foreground material is the permafrost table with the overlying active-layer removed, exposing the bowl-shaped depression in the permafrost table beneath the hummock. The active layer thickness is about 50 cm in the centre of the hummock and about 15 cm at the margins of the hummock where the organic soil horizon meets the permafrost table. The central lighter coloured mineral soil is clay-rich. Note the thick layer of vegetation and organic soil covering the top of the hummock.

Table 1. Terminology for zonal patterned-ground features on fine-grained soils of zonal sites mapped along the North American Arctic Transect (Raynolds et al. 2008). The terms are based on the morphology and size of the features and do not consider their genetic origin. Where possible, we followed Washburn's approach to classifying patterned ground (Washburn 1980) supplemented with the more recent glossary of permafrost and related ground-ice terms (van Everdingen 1998).

Feature	Definition	Subtype	Typical dimensions
Nonsorted Polygons	Polygonal forms without a border of stones, delineated by a crack or trough between adjacent polygons	Small	10–30 cm diam.
		Medium	30–200 cm diam.
Nonsorted Circles	Circular forms without a border of stones. Less vegetated in centers, and more vegetated on margins (synonyms include mud boils, frost boils, frost medallions, spotted tundra)	Small	10–50 cm diam.
		Medium	50–200 cm diam.
		Large	> 200 cm diam.
Hummocks	Dome-shaped features with a raised center and depression or trough between hummocks	Small	15–30 cm diam. 10–20 cm high
		Medium	100–200 cm diam. 30–60 cm high

dilation cracking, salt cracking, seasonal frost cracking, permafrost cracking, primary frost sorting, mass displacement, differential frost heaving and differential thawing (Washburn 1980), but more recent studies cited above indicate that vegetation may also play an important role in the genesis of these features.

The 'Biocomplexity of Patterned-Ground Ecosystems' project specifically examined the interactions between vegetation and physical components of patterned-ground ecosystems along the North America Arctic Transect (NAAT) (Walker et al. 2008a). We focused on non-sorted patterned-ground of zonal habitats in an attempt to avoid the complications involved with patterned-ground formation on slopes, rocky terrain and in wetlands. *Zonal* refers to vegetation and soils that develop on mesic, fine-grained soils under the influence of the regional climate, without the confounding influences of extremes of snow, site moisture, soil chemistry and texture, or major disturbances (Vysotsky 1909; Alexandrova 1980; Razzhivin 1999). The project focused on the hypothesis that as one moves from north to south along the gradient, changes in the thermal properties of the soils as a result of organic accumulation in different parts of the patterned-ground system result in gradients of soil moisture, active-layer thickness and frost heave across PGFs, and these in turn affect the size and shape of the features.

Other authors have developed conceptual models of the transformations of patterned-ground that can occur during vegetation succession. Matveyeva developed an eight-stage succession model for the formation of zonal plant communities based on detailed field observations and mapping of ecosystems along a climate gradient on the Taimyr Peninsula in Russia that included the full range of tundra from polar deserts to shrub tundra (Chernov & Matveyeva 1997). Shur developed a seven-stage model of earth-hummock development that portrays transformations of patterned-ground due principally to changes in the permafrost table (Shur et al. 2008).

This paper synthesizes information presented in two previous papers that described the vegetation along the

Low Arctic and High Arctic portions of the NAAT and a group of papers addressing biocomplexity in Arctic tundra (Kade et al. 2005; Vonlanthen et al. 2008; Walker et al. 2008b). A number of new, previously unpublished data sets regarding biomass, thermal properties of soils, spectral properties and interactions between vegetation and abiotic factors along the full gradient are included.

Study site locations

In 2001–2006 we studied patterned-ground landscapes at nine zonal Arctic locations in Canada and Alaska (Fig. 2). This report is confined to small patterned-ground features on zonal sites in the Arctic tundra, which is, for the most part, the region beyond the northern cold limit of forests (Walker et al. 2005). The locations were chosen as representative of zonal conditions within each of the five Arctic bioclimate subzones (CAVM Team 2003; Walker et al. 2005).

Much of our study focused on information from five core locations that were the most representative of the zonal situations: Isachsen (subzone A), Mould Bay (subzone B), Green Cabin (subzone C), Franklin Bluffs (subzone D) and Happy Valley (subzone E), but data are also included from all locations in the summary tables and figures. The brief descriptions below provide an overview of the variation along the gradient.

Geology

The Isachsen location was on clay-rich soils derived from marine shales of the Christopher Formation (Heywood 1957; Stott 1969). The Mould Bay location was located on soils derived from mixed sedimentary rocks of the Wilke Point and Griper Bay Formations (Everett 1968; Tedrow et al. 1968). The Green Cabin location was on mixed-textured glacial till deposited during the middle Pleistocene (Vincent 1982, 1990). In northern Alaska, the Howe Island, Deadhorse and Franklin Bluffs locations were on fine-grained soils derived from Sagavanirktok River loess (Everett & Parkinson 1977; Ping et al. 2008). The Sagwon

and Happy Valley locations were on weathered till of middle Pleistocene age or older that was covered with loess from the Sagavanirktok River (Hamilton 1986).

Vegetation

Floristically, the NAAT lies within the Northern Alaska and the Central Canada subprovinces of the Arctic and traverses all five bioclimate subzones (subzone A to subzone E, Fig. 2) of the Arctic zone (Yurtsev 1994). Bioclimate zonation is described in terms of characteristics of the vegetation and the mean July temperature (MJT) (Walker et al. 2005), i.e. Subzone A (cushion forb (*Papaver*) subzone), MJT = 0–3 °C; Subzone B (prostrate dwarf shrub (*Dryas*) subzone), MJT = 3–5 °C; Subzone C (hemiprostrate dwarf shrub (*Cassiope*) subzone), MJT = 5–7 °C; Subzone D (erect dwarf shrub (*Betula nana/exilis*) subzone), MJT = 7–9 °C; and Subzone E (low shrub (*Alnus*) subzone), MJT = 9–12 °C. The zonal vegetation along the NAAT varied from nearly barren surfaces with scattered bryophytes, lichens and very small forbs in subzone A to knee-high shrub-dominated tundra with thick moss carpets in subzone E. The plant communities on the associated zonal patterned-ground features are described in two previous papers: one described the Low Arctic Alaska part of the transect (Kade et al. 2005) and the other described the Canada High Arctic portion (Vonlanthen et al. 2008). A summary of the plant communities occur-

ring on and between patterned-ground features in each subzone and relevés used in our analysis is given in Appendix S1 (available online). A brief description of the vegetation at each of the core zonal locations follows.

The **Isachsen site** (subzone A) has sparse plant cover on a mesic, slightly south-facing slope. Cryptogam, herb barren vegetation (*Puccinellia angustata*–*Papaver radiculatum* comm.) occurs on the sparsely vegetated centres of PGFs and a rush/grass forb tundra (*Saxifraga*–*Parmelia omphalodes* ssp. *glacialis* comm.) is dominant between the PGFs (see Vonlanthen et al. 2008, Fig. 2b). There is a conspicuous absence of several plant groups that are abundant in all zonal sites further south, including sedges and plants with woody stems (i.e. dwarf shrubs). The **Mould Bay** (subzone B) site is near a hillcrest on a gentle slope with small, rounded non-sorted polygons (Vonlanthen et al. 2008, Fig. 3a). The tops of the polygons have discontinuous cover of crustose lichens (*Hypogymnia subobscura*–*Lecanora epibryon* comm.) and the inter-polygon areas have a graminoid, prostrate dwarf shrub, forb tundra (*Orthotrichum speciosum*–*Salix arctica* comm.). The **Green Cabin** (subzone C) site is in a low saddle on fine-grained sediments in an otherwise rocky upland landscape (Vonlanthen et al. 2008, Fig. 4b). The site has well-developed non-sorted circles that are nearly barren in the centres with prostrate dwarf shrub, herb tundra (*Dryas integrifolia*–*Carex rupestris* comm.) in areas between circles. The **Franklin Bluffs** (subzone D) site is on a flat, low old (estimated 2–5 kya) terrace of the Sagavanirktok River. The non-sorted circles are more vegetated than those at locations further north. The vegetation was divided into three primary plant communities: (1) *Junco biglumis*–*Dryadetum integrifoliae* typicum occurred in the more barren portions of the circles; (2) *Junco biglumis*–*Dryadetum integrifoliae pedicularietosum* was most common on partially vegetated margins of circles; and (3) *Dryado integrifoliae*–*Caricetum bigelowii* was dominant in the areas between circles (see Kade et al. 2005, Figs 10–12). The **Happy Valley** (subzone E) site is located on a gentle west-facing slope in the northern foothills of the Brooks Range. The vegetation is dominantly tussock tundra (*Sphagno-Eriophoretum vaginati*). The PGFs are not distinct because they are either covered by vegetation (*Cladino-Vaccinietum idaeae*) with abundant lichens, or they are small barren circles in wetter microhabitats hidden between tussocks (*Anthelia juratzkana*–*Juncus biglumis* comm.) (see Kade et al. 2005, Figs 13–15).

Methods

Climate

Air and ground temperatures and snow depth data were collected from stations established at each NAAT location

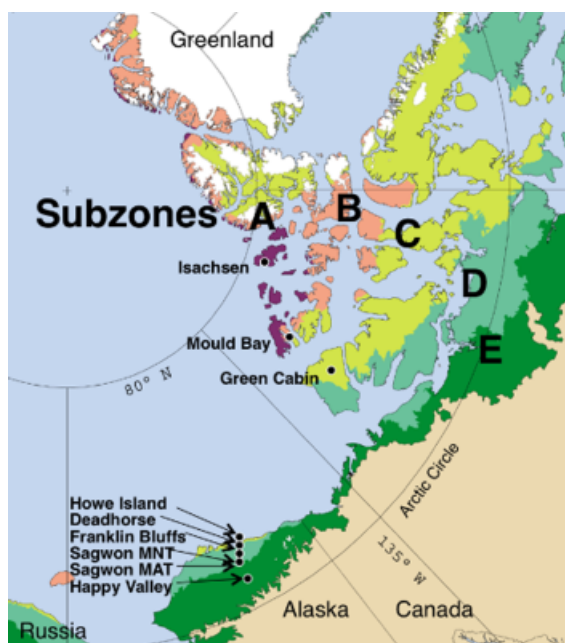


Fig. 2. Study locations along the North American Arctic Transect. The bioclimate subzones are from the Circumpolar Arctic Vegetation Map (CAVM Team 2003).

(Romanovsky et al. 2008). The installations are part of the Permafrost Observatory Network (Osterkamp 2003) and the Circumpolar Active Layer Monitoring Network (Brown et al. 2000). We use the summer warmth index (*SWI*) as a measure of total summer warmth: $SWI = \sum T_{mm}$, where T_{mm} is the mean monthly temperatures that exceed 0 °C and is expressed as thawing-degree months (°C mo). The index is easily derived from monthly mean temperatures and was first used to examine the temperature limitations of arctic plant species (Young 1971).

Sonic snow sensors attached to each climate station continuously measure snow depths. Snow depths were also measured manually during May 2006 (period of maximum snow depth) on all 1 × 1-m relevés and 10 × 10-m grids using a metal ruler. Green Cabin was not sampled manually because of hazardous landing conditions on the runway at the time of the survey. The missing data were substituted by sonic sensor data during that period. For each relevé, three to five measurements were averaged. Snow depths on the grids were recorded at 0.5 or 1.0 m intervals and visualized as maps (Raynolds et al. 2008).

Vegetation

Maps of study grids

The study focused on patterned-ground of flat zonal landscapes on fine-grained sediments. Twenty-one 10 × 10-m grids were mapped along the NAAT (Raynolds et al. 2008). The patterned-ground landscape within each grid was divided into three microhabitats where ever feasible: centres of patterned-ground features (PGF), relatively large vegetated intermediate areas around the margins of the PGFs (iPGF), and relatively undisturbed tundra between the patterned-ground features (bPGF). The mapped vegetation units characterize the plant communities growing on PGF, iPGF and bPGF microhabitats. For this paper, the map units were generalized to portray the dominant plant communities on the microhabitats.

Relevés

A total of 210 relevés were sampled, including 147 zonal relevés, which are synthesized here (Kade et al. 2005; Vonlanthen et al. 2008) (see Appendix S1 and S2). For the zonal areas, we retained the separation of the PGF, iPGF and bPGF communities. We also later combined the microhabitats within in each bioclimate subzone into 'zonal vegetation complexes'. One relevé of each community type was sampled within the mapped grids and four replicates were sampled from nearby tundra areas surrounding the grids. Plots were chosen subjectively to ensure that they were homogeneous, and as much as possible, floristically replicated the vegetation types that occurred on microhabitats

within the mapped 10 × 10-m grids. The size of the relevés varied. In the Low Arctic of Alaska, Kade et al. (2005) used 1-m² plots. In the High Arctic of Canada Vonlanthen et al. (2008) used variably sized plots. Many of microhabitats were very small and irregularly shaped; plots often contained more than one microhabitat and cover-abundance was visually estimated for the different microhabitats within the plot. It was generally not possible to use a standard size and shape of relevé frame. Instead an area of relatively homogeneous microhabitat was sampled in an increasingly large area until all the species were recorded. The size of the area sampled was then estimated at the end of the sampling. The minimum 1-m² area was sometimes not met within a single plot because the available homogeneous area of some PGF communities was < 1 m². In these cases, several adjacent small areas with similar vegetation were sampled so the total area approximated at least 1 m².

Vegetation data included in the analysis consisted of species composition (Br.-Bl. cover-abundance scores according to Westhoff & van der Maarel 1973), vegetation structure (canopy height and moss-layer height), cover of plant functional types (low shrubs, erect dwarf shrubs, prostrate dwarf shrubs, evergreen shrubs, deciduous shrubs, erect forbs, mat/cushion forbs, non-tussock graminoids, tussock graminoids, pleurocarpous bryophytes, acrocarpous bryophytes, liverworts, foliose lichens, fruticose lichens, crustose lichens).

Environmental variables

Data on soil chemical and physical properties were available for all 147 relevés (Kade et al. 2005; Vonlanthen et al. 2008). The soils were collected from the upper 10 cm of the topmost mineral horizon using a standard volume (190 cm³) soil can and analysed according to the USDA-NRCS procedures (USDA 1996). Soil chemical parameters measured were pH, total carbon content (total C), total nitrogen content (total N), cation exchange capacity (CEC) and availability of distinct cations (K⁺, Na⁺, Ca²⁺, Mg²⁺). Soil physical properties recorded were depth of organic horizon, depth of A horizon, bulk density, texture (percentage sand, silt and clay), gravimetric and volumetric soil moisture.

Other site factors were elevation, aspect, slope, snow duration, percentage of bare soil, percentage of salt crust, percentage of standing water, site moisture, glacial history, topographic position, site stability, wind exposure, maximum active layer thickness and maximum snow depth. Environmental and soil data used in the analyses are in Appendices S3a and S3b.

Biomass, NDVI and LAI

Biomass was sampled for 175 of the 210 relevés, with a minimum of five samples per plant community type per

location (see Appendix S4). Harvests were conducted at the time of peak biomass, early to mid-August, using a 20 × 50-cm frame. The samples were frozen prior to analysis and then sorted according to seven plant functional types (deciduous shrubs, evergreen shrubs, graminoids, forbs, horsetails, lichens, bryophytes). Biomass samples of deciduous and evergreen shrubs were subdivided into stem, live leaf, dead leaf and flower/fruit biomass. For graminoids, we separated live and attached dead biomass fractions. Samples were dried at 72 °C, weighed and measurements standardized to g m⁻².

To calculate landscape-level biomass of vegetation complexes, the biomass of the vegetation types were weighted by the percentage areas of vegetation units on the vegetation maps of the zonal grids then summed for each 100-m² map area.

The NDVI is an index of vegetation greenness and is a commonly used method of extrapolating biomass information to larger regions and has been used extensively in the Arctic as an index of a variety of key biophysical properties, including leaf area index (LAI), biomass and CO₂ flux (Stow et al. 2004). Green plants have high reflectivity in the near-infrared wavelengths and absorb red wavelengths for photosynthesis. $NDVI = (NIR - VIS) / (NIR + VIS)$, where NIR is the reflectance of the Earth's surface in the near-infrared channel (0.725 to 1.1 µm) and VIS is the reflectance in the visible portion of the spectrum or the red channel (0.5 to 0.68 µm) (Tucker & Sellers 1986).

NDVI and LAI data were collected at each of the field sites along the NAAT between the years 2000 and 2006. Hand-held NDVI was measured with a personal spectrometer (PS II (Analytical Spectral Devices, Boulder, CO, USA), and leaf area index was measured with a LAI-2000 Plant Canopy Analyser (LI-COR, Lincoln, NE, USA). Two 50-m transects were set in place at the zonal grids for each of the NAAT field sites (except for Howe Island – see below), with each transect encompassing one edge of the 10 × 10-m sampling grid. NDVI and LAI measurements were taken every meter along the transects. For the NDVI measurements, the optical sensor was held at nadir at 90 cm above the ground surface. The 25° field of view fibre-optic at 90 cm produces a circular footprint of ~0.125 m². For each LAI measurement, one above-canopy reading was taken along with four below-canopy readings, one in each of the cardinal directions 20 cm from the transect point.

In 2005, we began taking NDVI measurements for each of the relevés. We sampled 11 relevés at Isachsen in 2005 and 78 relevés on the North Slope in 2006 (including 15 relevés at Howe Island). We do not yet have NDVI for the relevés at Green Cabin or Mould Bay. We additionally acquired Advanced Very High Resolution Radiometer

(AVHRR) NDVI from the Large Area Coverage (LAC) data set for 1995 for the 1-km² pixel encompassing each of the sites; annual peak NDVI values from bi-monthly composites were extracted from the data set. We analysed the relationship between zonal above-ground biomass and hand-held NDVI along the NAAT. Hand-held NDVI values were averaged across all of the transect measurements for each of the sites, while above-ground biomass values for each zonal grid were taken from Reynolds et al. (2008). For Howe Island (where transect data were not available), we used the relevé NDVI data to calculate NDVI for three dominant land-cover types: bare ground, patterned ground-features (PGF) and tundra between patterned ground-features (bPGF). The fractional area coverage for each of these land-cover types on the zonal Howe Island grid were also taken from Reynolds et al. (2008), and the weighted average of NDVI for the Howe Island grid was calculated. We also analysed the relationships between summer warmth index (SWI = °C mo) and AVHRR-NDVI, hand-held NDVI and LAI along the NAAT. For the hand-held NDVI and LAI, values were the averages of all of the transect and relevé data for each of the sites.

Vegetation analysis

The Braun-Blanquet approach was used for sampling and classifying the vegetation (Westhoff & van der Maarel 1973). The approach has been applied to numerous areas in the Arctic. (See reviews in Walker et al. 1994a; Daniëls et al. 2005.) We combined the two zonal relevé data sets from Alaska and Canada in a Turboveg database (Hennekens & Schaminée 2001) containing 147 relevés and updated the nomenclature according to the Pan Arctic Flora Checklist (Elven et al. 2007). We added the updated environmental data including soil data, NDVI, LAI, biomass, climate, snow depth and active-layer thickness measurements.

We performed a Braun-Blanquet sorted table analysis using the software JUICE 6.5 (Tichý 2002). A frequency synoptic table was constructed for 'zonal vegetation complexes', which combined the data from PGF, bPGF and iPGF communities into a single community complex for each subzone. The table displays the frequency of diagnostic plant taxa in each zonal community complex. Only species with high fidelity for a given group and total frequencies > 20% are listed. Fidelity is used here as the occurrence concentration of species in relevés of a particular group compared to the group of other relevés in the table (Tichý & Chytrý 2006), and here is a numeric expression of the diagnostic value of a species for a given zonal complex. The fidelity of species was calculated using the phi (φ) coefficient (Tichý & Chytrý 2006). Phi can theoretically vary from -1 (the species occurs in all

relevés outside of the target group but none within the target group) to +1 (the species occurs in all relevés within the target group and no relevés outside the target group). Diagnostic species were subjectively selected as those with $\Phi \geq 0.55$; those with $\Phi \geq 0.8$ were considered highly diagnostic. The value of Φ depends partially on the ratio of the number of relevés within the group to the total number of relevés, so the size of the groups was first virtually equalized using the standardization function in JUICE. The statistical significance of Φ for all listed taxa is $P < 0.001$ using the Fisher's exact test (Tichý & Chytrý 2006).

For the ordination analysis, we retained the separate communities and calculated multivariate statistics (non-metric multidimensional scaling [NMDS] with the VEGAN community ecology package for R (R package version 1.17-4. Available at: <http://CRAN.R-project.org/package=vegan>). We chose NMDS technique as it does not assume unimodal species response curves and derives configuration scores only from the rank order of the dissimilarities between samples or species. It is therefore better suited for ecological data sets with a mix of continuous metrics of varying degrees of normality and homogeneity. For the final calculations we used the following specifications: (a) Braun-Blanquet cover-abundance scores transformation: $r = 1\%$, $+$ = 2%, $1 = 3\%$, $2 = 13\%$, $3 = 38\%$, $4 = 68\%$, $5 = 88\%$; (b) distance measure: Bray-Curtis; (c) number of dimensions: $k = 2$; (d) data auto-transformation: Wisconsin double transformation; (e) number of random starts: 20; (f) proportion of site pairs with no shared species to trigger stepacross function (=proportion of site pairs with no shared species): 0.1; (g) site parameter fitting based on 1000 permutations omitting missing values; (h) post-processing: vector rotation according to principal components analysis.

Soil thermal properties, n -factor, active layer and frost heave

We used the n -factor to elucidate the thermal (insulative) properties of vegetation and organic matter above the soil within and between PGFs (Kade et al. 2006). The n -factor is an indicator of the energy balance at the ground surface; it was developed in arctic engineering studies to estimate temperatures of homogeneous artificial surfaces from air temperatures (Carlson 1952). It is calculated as the ratio of seasonal thawing or freezing degree-day sums at the soil surface to that in the air. In summer, an n -factor uses thawing degree-days, and a value greater than 1 indicates that the mean soil-surface temperature is greater than the air temperature, and when it is less than 1 the soil temperature is less than the air temperature. In winter, n is calculated using freezing degree-days, and in this case, an n -factor less than 1 indicates that the soil-

surface temperature is warmer than the air temperature. Recently, n -factors have been calculated for natural systems to assess the surface thermal regime under a variety of natural vegetation types (Klene et al. 2001b; Taylor 2001; Karunaratne & Burn 2003), and used in models to estimate permafrost temperatures and active-layer thickness over large areas (Klene et al. 2001a). Here, we compare the air temperature to (1) that at the soil surface just below live vegetation (sometimes this at the top of the organic soil horizons) and (2) below the soil organic horizon at the top mineral soil surface. The n -factors of this study are site-specific and depend on the thickness and type of vegetation present and snow cover during winter. We determined summer and winter n -factors.

A total of 175 iButton (Maximum Integrated Products Inc.) loggers were located within 107 relevés – at the soil surface (PGF) and (if present) at the interface between organic and mineral soil. Daily mean temperatures were obtained for air, the base of live vegetation and the top of the uppermost mineral soil horizon. Thawing degree-day sums for the air (TDD_a), live vegetation (TDD_v) and the top of the mineral soil surface (TDD_m) were calculated by summing daily mean temperatures from the first to the last day of the season that the mean soil surface temperature rose above 0°C . Similarly, freezing degree-day sums were determined for air (FDD_a), live vegetation (FDD_v) and the mineral soil surface (FDD_m) by summing daily mean temperatures from the first to the last day of the season that the mean soil surface temperature dipped below 0°C . The following n -factors were determined for each study plot: Summer n -factor for live vegetation: $n_v = TDD_v/TDD_a$; summer n -factor at the mineral soil surface: $n_m = TDD_m/TDD_a$; winter n -factor for live vegetation: $n_v = FDD_v/FDD_a$; and winter n -factor at the mineral soil surface: $n_m = FDD_m/FDD_a$. For details of the n -factor analysis for the Low Arctic see Kade et al. (2006), which includes n -factors for the Alaska portion of the NAAT. Readings for the Canadian sites were not available previously and this synthesis now completes the analysis of the patterned-ground thermal regimes along the NAAT.

Active-layer thickness (depth to the permafrost) data for relevés and grids were collected using a 1-m long graduated metal probe (Nelson et al. 1996). End-of-growing-season thaw data were collected from all sites in 2006. For each relevés, three to five measures were averaged. Active-layer thickness was also recorded at 0.5- or 1-m intervals for the grids and visualized as maps (Raynolds et al. 2008).

Frost heave was measured adjacent to the 20 grids with ten-pin heavometers (Alaska portion of NAAT) or single-bar devices with vertically moving metal plates [some in Alaska and all Canada sites (Romanovsky et al. 2008)]. Same-year readings were not available for all sites but

numerous data sets from different site combinations and years were available. Heave data were collected prior to the spring thaw.

Results

Climate

Complete summaries of the environmental and soil data are in Appendices S3a and S3b (available online). Thawing degree-days (TDD) showed a nearly linear ten-fold increase along the NAAT from about 100 TDD in subzone A to 1100 TDD in subzone E (Fig. 3a). Temperatures at the top of the mineral soil surface in the centres of PGFs were somewhat higher than the air temperature in subzones A, B, C, about the same as the air temperature in subzone D, and considerably less than the air temperature in subzone E. The mineral soil temperatures in the bPGF microhabitats were statistically the same as the air temperatures in subzones A, B and C, and were much lower than the air temperatures in subzones D and E, where there are thick organic soil horizons. The temperature at the top of the mineral soil in bPGF habitats in subzone E was about the same as in subzone A (about 100 TDD).

Freezing degree-days (FDD) ranged from about 6000 FDD in subzones A and B to about 4500 FDD in subzone C (Fig. 3b). Winter FDD total at the top of the mineral soil horizons for the PGF and iPGF microsites were close to the air total in subzone A, B and C. Winter mineral soil temperatures were much warmer than the air temperatures in subzones D and E. In subzones D and E, soil temperatures were considerably colder than the air temperatures in summer and much warmer than the air temperatures in winter. The colder winter air temperatures in subzones D and E reflect the more continental study locations in these subzones.

Snow depths between PGFs in the far north (subzones A and B) were in the range of 20 to 25 cm (Fig. 3c). The shallowest snow was in subzone C (about 5–10 cm), and increased to about 35 cm in subzone D and 73 cm in subzone E. Snow depths were generally deeper between PGFs than on the tops of the features, but it was not always possible to accurately locate the features beneath the snow, particularly the small non-sorted polygons of subzones A and B.

Soils

Despite the substrate variation, most soil textures along the gradient were loams to sandy loams, in accordance with our desire to locate plots in zonal loamy sites (Appendix S5, available online). The exceptions were clay soils at Isachsen (subzone A), which were a product of weathering of the Christopher Formation shale deposits. The rationale for selecting loamy sites was that such sites better fit the zonal concept and fine-grained soils with high silt content heave more than coarser grained sediments and are thus more likely to have well-developed patterned-ground features (Peterson & Krantz 2003).

The strongest contrast in the soil textures of microhabitats within a subzone occurred in subzones C and D, where the non-sorted circles were best developed and there was likely some sorting of the sediments due to frost heave.

The Happy Valley soils were acidic ($\text{pH} < 5.5$) in the uppermost mineral horizon and all the others were non-acidic. Several sites (Howe Island, Green Cabin, Deadhorse, Franklin Bluffs) had a soil pH exceeding 8.0. Total soil organic carbon values determined from the upper 1 m of soil in the soil pits were 15.2 kg m^{-3} at Isachsen, 21.1 kg m^{-3} at Mould Bay, 27.6 kg m^{-3} at Green Cabin, 60.8 kg m^{-3} at Franklin Bluffs and 57.8 kg m^{-3} at Happy

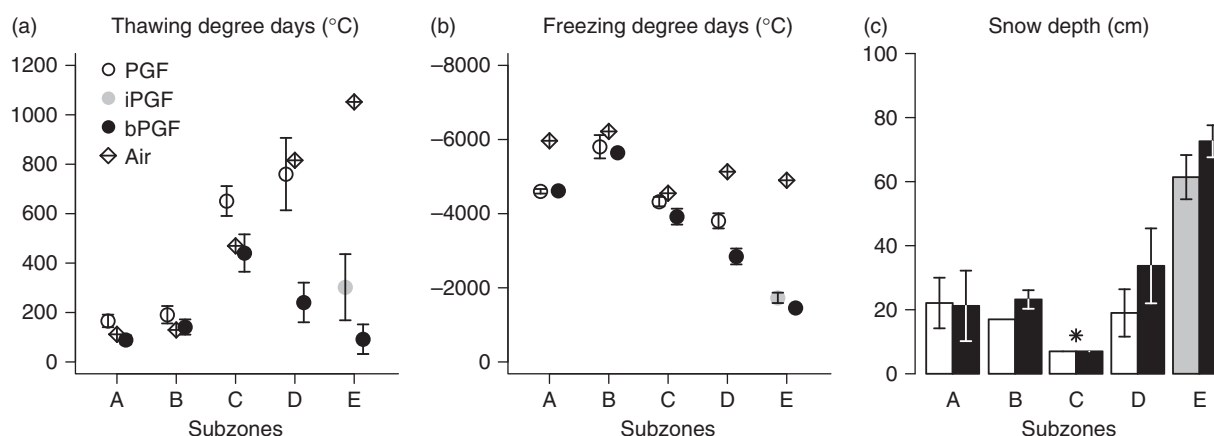


Fig. 3. Key climate properties along the NAAT. (a) Thawing degree-days ($^{\circ}\text{C}$); (b) freezing degree-days ($^{\circ}\text{C}$); (c) snow depth (cm). White: barren or sparsely vegetated centres of patterned-ground features (PGF), black: continuous vegetation between patterned-ground features (bPGF). Error bars = standard deviation. Asterisk = values derived from sonic snow sensors (for details see text).

Valley. Soil carbon values were higher than expected in the High Arctic (subzones A, B, C), but generally below 30 kg m^{-3} , whereas values above 55 kg m^{-2} occurred in the Low Arctic (see Ping et al. (2008) and Michaelson et al. (2008) for more complete information regarding the soils along the NAAT).

Vegetation

Synoptic table of zonal vegetation complexes

Association tables for the plant communities occurring in the various patterned-ground microhabitats have been published previously (Kade et al. 2005; Vonlanthen et al. 2008).

The synoptic table of zonal vegetation complexes displays the diagnostic taxa identified according the phi-coefficient criteria used ($\Phi \geq 0.55$, diagnostic taxa (highlighted); $\Phi \geq 0.8$, highly diagnostic taxa (highlighted in dark grey) (Table 2). Groups of diagnostic taxa are listed for each zonal vegetation complex and ordered from highest to lowest phi coefficient.

A clear set of diagnostic taxa occurs for each of the subzones, except subzone C. The zonal complexes at the north and south ends of the climate gradient had large numbers of diagnostic species. Subzone A had the largest number (34); 21 of these were lichens; nine were vascular plants and four were bryophytes. Highly diagnostic taxa included *Pertusaria octomela*, *Psoroma hypnorum*, *Rinodina terrestris*, *Draba oblongata* and *D. subcapitata*. Subzone E had 25 diagnostic taxa, seven vascular plants, nine lichens and eight bryophytes; and seven highly diagnostic taxa including *Betula nana*, *Vaccinium vitis-idaea*, *Cladina rangiferina*, *Petasites frigidus*, *Dicranum elongatum*, *C. arbuscula* and *Empetrum nigrum*. Subzone B had 13 diagnostic taxa, subzone C had three and subzone D had 17. The few diagnostic taxa in subzone C was related to the generally depauperate nature of patterned-ground features at the two subzone-C locations, and the locations were in different floristic subprovinces, which limited the broader occurrence of a few of the taxa. A few common species that might be expected to be diagnostic within individual subzones appear lower in the table where diagnostic taxa are listed for groups of subzones. For example, *Papaver radicum*, *Alopecurus alpinus*, *Saxifraga cespitosa* and *Poa abbreviata* are very common in the High Arctic and are listed as diagnostic for the larger area of subzones A and B. Similarly, *Dryas integrifolia*, *Saxifraga oppositifolia* and *Salix arctica* are some of the most common species in the middle part of the Arctic and are listed as diagnostic for the group of subzones B, C and D. The species *Polygonum viviparum*, *Tephrosia atropurpurea*, *Eriophorum vaginatum*, *Arctagrostis latifolia* and *Carex bigelowii* are very common on zonal sites

in the Low Arctic and are listed as diagnostic for subzones D and E.

The plant taxa in Table 2 are diagnostic only against the set of zonal communities represented in Table 3, but are broadly characteristic of zonal sites within the bioclimate subzones of northern Alaska and northwestern Canada. Samples from a wider region are needed to develop a better picture of differential and characteristic taxa for zonal patterned-ground complexes across Arctic North America, particularly the High Arctic. Information from a wider geographic range of zonal locations should be collected before naming zonal associations in the sense that Matveyeva (1998) has done for the Taimyr Peninsula in Russia.

Ordination of vegetation in relationship to environmental gradients

The zonal complexes are displayed as ellipses in the NMDS ordination (Fig. 4a). The primary criterion for the arrangement of the plots in the NMDS diagram is floristic dissimilarity of the relevés. The biplot diagram in Fig. 4b displays the direction and strength of the primary environmental gradients. The length of the vector indicates the strength (R^2 , Table 3) of the correlation between the environmental variable and position of the relevés along the gradient. Vectors with $R^2 > 0.2$ are displayed.

The zonal complexes of plant communities were well separated in the NMDS ordination. The diagram can be split into Canada and Alaska portions, separated by the dashed line in Fig. 4a. The Canada subzones are arranged from cold to warm (A to C) along the Y-axis, and the Alaska group is arranged in the opposite direction from cold to warm (C to E) along a diagonal from the upper left to the lower right of the ordination. The larger number of relevés in the Alaska portion of the NAAT influences the ordination and the direction of the arrows in the biplot diagram (Fig. 4b). For example, the direction of the summer warmth vector (SWI) corresponds most clearly with the climate trend of the Alaska portion of the ordination. Also, the biomass gradients (dashed lines in the lower biplot diagram) do not reflect biomass trends for the Canadian portion of the transect. The differences in the regional floras in Alaska versus Canada also influence the ordination. A few species common in parts of the Beringian Northern Alaska floristic subprovince are missing in the Central Canada floristic subprovince, including *Salix ovalifolia*, *Oxytropis borealis*, *Parrya nudicaulis*, *Sausurea angustifolia* and *Braya glabella* ssp. *purpurascens*. Similarly, *Parrya arctica* and *Oxytropis arctobia* are common in parts of Canada but missing in Alaska (Yurtsev 1994).

Within the subzone groups, the microhabitats are separated in a generally consistent way in Fig. 4. In

Table 2. Synoptic table of zonal vegetation complexes (includes relevés on and between patterned-ground features) along the North American Arctic Transect. Values are frequency of the given plant taxon within the indicated zonal complex. Fidelity of diagnostic species was calculated using the phi coefficient for individual subzones and groups of two or three adjacent subzones. Diagnostic species were subjectively selected as those with $\Phi \geq 0.55$ and are highlighted; those with $\Phi \geq 0.8$ are considered highly diagnostic and are highlighted with dark gray. Species are ordered according descending fidelity. Only species with frequencies > 20% are listed. Second column: B, Bryophyte; L, Lichen; V, Vascular plant.

Subzone		A	B	C	D	E
No. of relevés:		21	10	29	62	25
No. of species:		142	79	108	226	108
Diagnostic taxa for subzone A						
<i>Pertusaria octomela</i>	L	90
<i>Psoroma hypnorum</i>	L	86	.	.	.	4
<i>Rinodina terrestris</i>	L	76
<i>Draba oblongata</i>	V	95	.	24	.	.
<i>Draba subcapitata</i>	V	71
<i>Cardamine bellidifolia</i>	V	67
<i>Poa alpigena</i>	V	67
<i>Ranunculus sabinei</i>	V	67
<i>Saxifraga cernua</i>	V	76	30	.	.	.
<i>Cerastium arcticum</i>	V	76	30	.	.	.
<i>Rinodina turfacea</i>	L	86	20	.	6	4
<i>Racomitrium panschii</i>	B	71	20	.	.	.
<i>Peltigera didactyla</i>	L	71	.	.	3	.
<i>Syntrichia ruralis</i>	B	90	50	21	.	.
<i>Fuscopannaria praetermissa</i>	L	62
<i>Puccinellia cf. andersonii</i>	V	62
<i>Lecidella wulfenii</i>	L	62
<i>Caloplaca ammiopila</i>	L	62	10	.	.	.
<i>Festuca brachyphylla</i>	V	57
<i>Schistidium frigidum</i>	B	57
<i>Protopannaria pezizoides</i>	L	57
<i>Megalania jemtländica</i>	L	52
<i>Stereocaulon rivulorum</i>	L	48
<i>Tetramelas insignis</i>	L	48
<i>Schistidium papillosum</i>	B	52	20	.	.	.
<i>Ochrolechia inaequatula</i>	L	57	10	.	3	4
<i>Candelariella terrigena</i>	L	43
<i>Megaspora verrucosa</i>	L	67	30	21	2	.
<i>Caloplaca cerina</i>	L	52	20	3	2	.
<i>Peltigera canina</i>	L	43	.	.	2	.
<i>Rinodina olivaceobrunnea</i>	L	38
<i>Sticta arctica</i>	L	38
<i>Ochrolechia cf. inaequatula</i>	L	38
<i>Cladonia pyxidata</i>	L	62	.	.	13	8
Diagnostic taxa for subzone B						
<i>Oxyria digyna</i>	V	.	90	.	.	.
<i>Potentilla hyparctica</i>	V	57	100	.	.	.
<i>Orthotrichum speciosum</i>	B	5	70	.	.	.
<i>Luzula nivalis</i>	V	33	90	.	.	16
<i>Festuca hyperborea</i>	V	.	60	.	.	.
<i>Draba sp.</i>	V	.	70	21	.	.
<i>Parrya arctica</i>	V	.	80	41	.	.
sterile black crust	L	.	50	.	.	.
<i>Lecidea ramulosa</i>	L	.	50	.	.	.
<i>Bryum rutilans</i>	B	.	50	.	2	.
<i>Didymodon rigidus</i> var. <i>icmadophila</i>	B	43	80	17	5	0
<i>Ctenidium procerrimum</i>	B	.	80	48	6	.
<i>Mnium thomsonii</i>	B	.	40	.	.	.
Diagnostic taxa for subzone C						
<i>Puccinellia angustata</i>	V	.	.	55	.	.

Table 2. Continued

Subzone		A	B	C	D	E
No. of relevés:		21	10	29	62	25
No. of species:		142	79	108	226	108
<i>Braya glabella</i> ssp. <i>purpurascens</i>	V	.	.	48	2	.
<i>Oxytropis borealis</i>	V	.	.	38	.	.
Diagnostic taxa for subzone D						
<i>Eriophorum angustifolium</i> ssp. <i>triste</i>	V	.	.	.	100	.
<i>Carex membranacea</i>	V	.	.	.	81	.
<i>Cardamine digitata</i>	V	.	.	.	73	.
<i>Salix reticulata</i>	V	.	.	.	68	.
<i>Equisetum variegatum</i>	V	.	.	.	65	.
<i>Hypnum bambergeri</i>	B	.	.	14	79	.
<i>Carex capillaris</i>	V	.	.	.	56	.
<i>Thamnolia subuliformis</i>	L	.	.	28	89	4
<i>Tofieldia pusilla</i>	V	.	.	.	50	.
<i>Pedicularis lanata</i>	V	.	.	.	58	8
<i>Arctous rubra</i>	V	.	.	.	48	4
<i>Astragalus umbellatus</i>	V	.	.	.	40	.
<i>Equisetum arvense</i>	V	.	.	.	40	.
<i>Pedicularis capitata</i>	V	.	.	.	44	.
<i>Carex scirpoidea</i>	V	.	.	.	35	.
<i>Catoscopium nigrum</i>	B	.	.	.	35	.
<i>Papaver macounii</i>	V	.	.	.	35	.
Diagnostic taxa for subzone E						
<i>Betula nana</i>	V	100
<i>Vaccinium vitis-idaea</i>	V	.	.	.	2	100
<i>Cladina rangiferina</i>	L	84
<i>Petasites frigidus</i>	V	84
<i>Dicranum elongatum</i>	B	.	.	.	5	92
<i>Cladina arbuscula</i>	L	76
<i>Empetrum nigrum</i>	V	.	.	.	3	80
<i>Cladina stygia</i>	L	64
<i>Cladonia amaurocraea</i>	L	.	.	.	6	72
<i>Sphenobolus minutus</i>	B	14	.	.	3	80
<i>Aulacomnium turgidum</i>	B	48	.	.	15	100
<i>Hylocomium splendens</i>	B	14	10	14	15	96
<i>Cassiope tetragona</i>	V	.	.	.	31	96
<i>Pedicularis lapponica</i>	V	52
<i>Salix pulchra</i>	V	52
<i>Pleurozium schreberi</i>	B	.	.	.	2	52
<i>Cladonia fimbriata</i>	L	.	.	.	2	52
<i>Dactylina arctica</i>	L	.	.	3	31	92
<i>Dicranum acutifolium</i>	B	5	.	.	3	56
<i>Dicranum groenlandicum</i>	B	40
<i>Peltigera leucophlebia</i>	L	29	.	.	5	64
<i>Cetraria laevigata</i>	L	.	.	.	3	44
<i>Peltigera malacea</i>	L	.	.	.	2	40
<i>Sphagnum warnstorffii</i>	B	36
Diagnostic taxa for subzones A and B						
<i>Papaver radicum</i>	V	100	80	.	.	.
<i>Alopecurus alpinus</i>	V	90	90	.	.	.
<i>Hypnum revolutum</i>	B	95	80	14	.	.
<i>Parmelia omphalodes</i> ssp. <i>glacialis</i>	L	81	50	.	.	.
<i>Polytrichastrum alpinum</i>	B	76	60	.	.	.
<i>Saxifraga nivalis</i>	V	67	60	.	.	.
<i>Pohlia cruda</i>	B	62	50	.	.	.
<i>Stellaria longipes</i>	V	76	80	17	3	.
<i>Saxifraga cespitosa</i>	V	43	70	.	.	.
<i>Sanionia uncinata</i>	B	43	80	.	2	.

Table 2. Continued

Subzone		A	B	C	D	E
No. of relevés:		21	10	29	62	25
No. of species:		142	79	108	226	108
<i>Poa abbreviata</i>	V	43	60	.	.	.
<i>Timmia austriaca</i>	B	57	70	3	5	.
Diagnostic taxa for subzones B and C						
<i>Fulgensia bracteata</i>	.	.	50	45	.	.
Diagnostic taxa for subzones B, C and D						
<i>Dryas integrifolia</i>	V	.	100	48	98	.
<i>Saxifraga oppositifolia</i>	V	.	100	55	68	.
<i>Salix arctica</i>	V	.	90	66	53	4
Diagnostic taxa for subzones C and D						
<i>Polyblastia sendtneri</i>	L	.	.	28	45	.
Diagnostic taxa for subzones D and E						
<i>Bistorta vivipara</i>	V	.	.	21	95	100
<i>Tephrosia atropurpurea</i>	V	.	.	.	68	60
<i>Eriophorum vaginatum</i>	V	.	.	.	48	64
<i>Arctagrostis latifolia</i>	V	.	.	3	53	56
<i>Carex bigelowii</i>	V	.	.	.	29	60
Nondiagnostic but common taxa occurring in more than 20% of the relevés						
<i>Ditrichum flexicaule</i>	B	71	80	45	95	32
<i>Flavocetraria cucullata</i>	L	5	100	10	68	96
<i>Cetraria islandica</i>	L	57	100	.	74	48
<i>Distichium capillaceum</i>	B	52	80	34	81	.
<i>Tomentypnum nitens</i>	B	24	50	14	77	32
<i>Cladonia pocillum</i>	L	67	30	7	66	4
<i>Lecanora epibryon</i>	L	14	50	55	53	.
<i>Thamnolia vermicularis</i>	L	76	100	31	11	60
<i>Solorina bispora</i>	L	24	.	14	53	.
<i>Flavocetraria nivalis</i>	L	.	10	.	48	28
<i>Distichium inclinatum</i>	B	10	60	21	34	.
<i>Juncus biglumis</i>	V	.	50	3	47	.
<i>Campylium stellatum</i>	B	5	.	17	45	.
<i>Rinodina roscida</i>	L	5	40	38	23	.
<i>Orthothecium chryseum</i>	B	10	40	.	39	.
<i>Hulteniella integrifolia</i>	V	.	.	31	34	.
<i>Minuartia arctica</i>	V	.	.	14	42	.

Canada, the more barren PGF microhabitats are situated to the right and above the bPGF microhabitats, and the iPGF microhabitats are situated between the two. In the Alaska portion of the diagram, the PGF microhabitats are arranged more directly above the iPGF and in subzone E there is little floristic separation between the microhabitats. The largest floristic contrast of microhabitats within a subzone is in subzone C, where there are also the largest differences of several ecological site factors between the dry barren centres of the features compared to the much more lush and more mesic tundra between the features, including soil moisture, soil temperature and active layer thickness. Species turnover from north to south was large, at over 5 SD units, indicating nearly completely dissimilar species groups at the ends of the gradients.

The ordination biplot revealed that summer warmth (expressed as SWI, $R^2=0.74$, Table 3) and soil pH

($R^2=0.73$) were the two dominant and independent environmental factors explaining vegetation composition (Fig. 4b). SWI ranged from 3.6 °C in the north to 30.2 °C in the south and thus covered almost the complete temperature range in the Arctic. Soil pH values ranged from 5.0 in subzone E to pH 8.0 in subzones D and C. The snow depth gradient ($R^2=0.6$) was parallel to the SWI gradient. The arrangement of the plots in the ordination space is strongly influenced by the opposing latitudinal directions of the pH gradients in Canada and Alaska. In Canada, pH varied from 6.1 to 6.5 at Isachsen in the north to 7.9 to 8.4 at Green Cabin in the south, whereas in Alaska the highest pH values were in the north – 7.9 to 8.6 at Howe Island compared to 4.8 to 5.2 at Happy Valley. The geological and soil differences between Canada (tills and clays) and Alaska (loess) also influence the floristic composition of the zonal vegetation.

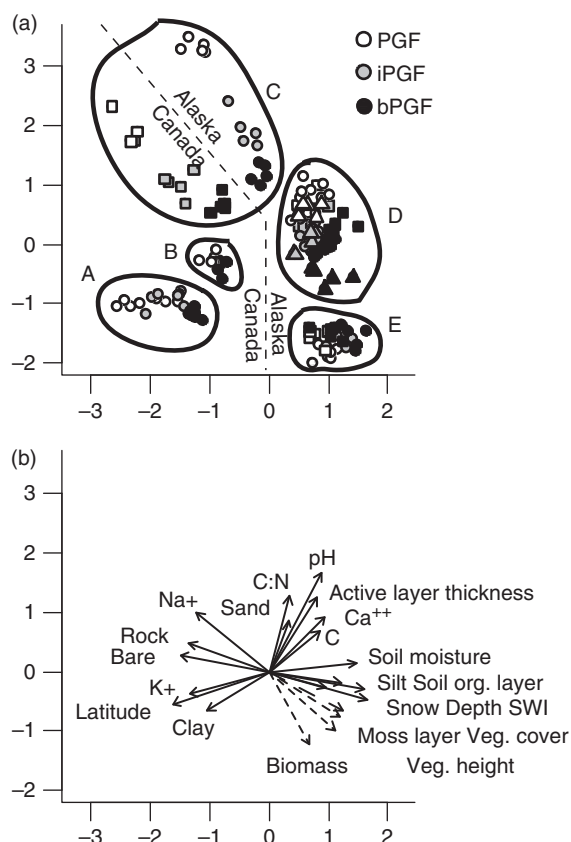


Fig. 4. Nonmetric Multi-Dimensional Scaling (NMDS) ordination of zonal vegetation along the NAAT. **(a)** Ordination of relevés based on plant species cover, grouped by bioclimate subzone. Shapes of symbols within each subzone correspond to locations: Subzone A: circles = Isachsen; Subzone B: circles = Mould Bay; Subzone C: circles = Howe Island, squares = Green Cabin; Subzone D: circles = Deadhorse, squares = Franklin Bluffs, triangles = Sagwon MNT; Subzone E: circles = Sagwon MAT, squares = Happy Valley. Dashed line separates the Alaska portion of the transect from the Canada portion. **(b)** Ordination biplot indicating direction and strength of the principal abiotic (solid lines) and biotic (dashed lines) gradients. Axes are labelled in half-change units so that one unit means halving of community similarity. Biplot vector cutoff value is 0.2.

A group of biomass-related variables (total biomass, plant canopy height, soil organic layer thickness, moss thickness, total vegetation cover, and moss cover) corresponded most closely to the summer warmth and snow gradients (dashed vectors in Fig. 4b).

Vegetation structure

Example vegetation maps from each subzone portray the general trend in horizontal structure of plant communities with respect to patterned ground along the NAAT (Fig. 5). In subzones A and B, the dominant PGFs were small, non-sorted polygons with tight mosaics of plant communities that corresponded to the centres of the

polygons and narrow cracks between the polygons. In subzones C, D and E, the mapped patterns were associated with non-sorted circles or earth hummocks that occupied larger horizontal spaces than the small polygons in subzones A and B. In subzones C and D there were distinctive intermediate plant communities (grey patterns in C and D of Fig. 5) between the predominantly barren centres of the features and the completely vegetated tundra between the PGFs. These plant communities were colonizing margins of the PGFs. In subzone E, non-sorted circles were not so apparent. Most of the circles were fully colonized by plant communities that structurally resembled those of the areas between the hummocks.

The height of the vascular plant canopy on the patterned-ground features increased from 1 cm at Isachsen to 13 cm at Happy Valley (Fig. 6a, white bars in A–D, grey bar in E). The height of the vascular plant canopy between the PGFs increased from 1 cm at Isachsen to 21 cm at Happy Valley (Fig. 6a, black bars).

In general PGF microhabitats had low biomass ($< 25 \text{ g m}^{-2}$) in subzones A, B and C. Forb, graminoid and evergreen shrub biomass increased somewhat on PGF microhabitats in subzone D (above 25 g m^{-2}). In subzone E, the PGF microhabitats had high biomass of several plant growth forms (bryophytes, lichens, graminoids, deciduous shrubs and evergreen shrubs) (Fig. 6b). Above-ground biomass on the centres of the PGFs varied 19-fold, from 39 g m^{-2} at Isachsen (subzone A) to 734 g m^{-2} at Sagwon MAT (subzone E), versus about a twofold increase in biomass of the vegetation between PGFs (369 g m^{-2} at Isachsen to 758 g m^{-2} at Sagwon MAT) (Fig. 6b). The high bryophyte biomass values in the bPGF microhabitats at Isachsen and Mould Bay (comparable to the corresponding microhabitats in subzones D and E) are suspect and are likely caused by windblown sand contamination, which has been noted in more recent biomass samples from High Arctic sites in Russia (Walker et al. 2009).

Some plant growth forms showed distinctive trends along the gradient. Deciduous and evergreen shrubs did not occur in subzone A. Evergreen shrub biomass peaked in bPGF microhabitats of subzone C (400 g m^{-2}) due to high cover of *Dryas integrifolia* and remained high ($100\text{--}200 \text{ g m}^{-2}$) in bPGF microhabitats of subzones D and E (in subzone E, the dominant evergreen shrubs were *Vaccinium vitis-idaea* and *Ledum decumbens*). High evergreen shrub biomass (about 250 g m^{-2}) also occurred on the PGF microhabitats in subzone E. Deciduous shrub biomass was low ($< 25 \text{ g m}^{-2}$) in PGF microhabitats along the entire gradient, but in bPGF habitats, deciduous shrubs showed a strong increasing trend with temperature, from less than 25 g m^{-2} in subzones B and C to about 50 g m^{-2} in subzone D, and over 100 g m^{-2} in subzone E. Other plant growth forms showed less distinctive trends along the gradient.

Table 3. Ordination biplot vectors for NMDS axis 1 (NMDS1) and 2 (NMDS2), correlation coefficient R^2 and significances. Significance thresholds. ***: $P < 0.001$.

	NMDS1	NMDS2	R^2
Latitude	0.99	-0.16	0.60***
Summer Warmth Index (SWI)	0.83	-0.56	0.74***
NDVI	0.74	-0.68	0.54***
Biomass (total above-ground)	0.89	-0.46	0.40***
Soil organic layer thickness	0.55	0.83	0.31***
Moss layer thickness	0.96	-0.28	0.41***
Vegetation height	0.47	0.88	0.46***
Vegetation cover	-0.95	0.31	0.41***
Active layer thickness	-0.99	0.17	0.46***
Snow depth	0.43	0.90	0.60***
pH	0.96	-0.26	0.73***
Rock cover	-0.85	-0.53	0.44***
Bare ground cover	0.71	0.70	0.48***
Sand content	-0.96	-0.28	0.23***
Silt content	-0.78	0.62	0.20***
Clay content	1.00	0.10	0.32***
Ca ²⁺ concentration	0.27	0.96	0.36***
K ⁺ content	0.78	0.62	0.40***
Na ⁺ content	0.99	-0.16	0.52***
Soil moisture	0.83	-0.56	0.45***
C:N ratio	0.74	-0.68	0.36***
Carbon content	0.89	-0.46	0.25***

Total landscape-level biomass, as calculated from the vegetation maps of zonal complexes, increased 4.3-fold along the gradient: 17 kg 100 m⁻² at Isachsen (subzone A), 15 kg 100 m⁻² at Mould Bay (subzone B); 30 kg 100 m⁻² at Green Cabin (subzone C), 43 kg 100 m⁻² at Franklin Bluffs (subzone D) and 73 kg 100 m⁻² at Happy Valley (subzone E) (Fig. 6c).

NDVI and LAI

AVHRR-derived NDVI was strongly and positively correlated with the summer warmth gradient and less strongly with landscape-level biomass ($R^2 = 0.92$ and 0.67 , respectively) (Fig. 7a and d); whereas the hand-held measurements of NDVI were strongly positively correlated with both SWI and total landscape-level above-ground biomass ($R^2 = 0.87$ and 0.85 , respectively) (Fig. 8b and e). This is logical because the hand-held measurements were taken in the immediate vicinity of the mapped grids from which the landscape-level NDVI values were derived, whereas the AVHRR-derived pixels cover 1-km² areas in the vicinity of the grids.

There was higher variability in hand-held NDVI at the colder sites because of a greater contrast of the green vegetation in the PGF versus bPGF microhabitats in the northern compared to the southern locations. LAI also showed a somewhat weaker correlation with SWI (Fig. 7c,

$R^2 = 0.68$) because the sensor on the LAI instrument was 2 cm above ground level and located above most of the plant canopy in the High Arctic locations. The correlation between LAI and biomass was quite strong (Fig. 7f, $R^2 = 0.86$).

n-factors, active-layer thickness and soil heave

The summer *n*-factors showed a pronounced differences between the northern part of the transect (subzones A, B and C) and the southern part (Fig. 8a). At all three northern sites, the *n*-factors on the tops of the PGFs were near 1.5, indicating that the sum of thawing degree-days at the ground surface was about 1.5 times that of the air. This was due to the nonexistent or thin cover of vegetation and bryophytes above the top mineral horizons and strong radiative warming of the ground. This is in contrast to the *n*-factor of the microhabitats between patterned-ground features in the High Arctic, which were near 1.0, demonstrating the thermal effect of thin bryophyte layers in these microhabitats. At low temperatures, small absolute differences between the daily mean temperatures of the air and ground surface result in the large relative differences, as reflected in the *n*-factor. For example, in subzone A, the TDD total for the PFG microhabitats is 180 °C days compared to 100 °C days in the iPGF microhabitats and 110 °C day for the air (Fig. 5a), yielding an *n*-factor of 1.6 for the PGFs and 0.9 for the iPGF microhabitats. In subzone C, the TDD total is about 650 °C days on PGF microhabitats and 450 °C days, yielding an *n*-factor of 1.4, and well reflects the biological impact of small differences in temperature near freezing point.

The thick organic soil and bryophyte layers in the bPGF microhabitats of subzones D and E caused very low summer *n*-factors at the top of the mineral soil – about 0.25 in subzone D and 0.1 in subzone E (Fig. 8a). The *n*-factors of the PGF microhabitats in subzone D were close to 1.0, substantially less than in the High Arctic because of the thin cover of vegetation, but much higher than the PGFs in subzone E, where the *n*-factors were close to 0.25, a reflection of the thick vegetation, usually exceeding 10–15 cm thick.

The winter *n*-factors in all subzones are below the 1.0 equilibrium line, i.e. soils were less cold on average than the air in both microhabitats (Fig. 8b). Also, there was little difference between PGF and bPGF within a location during winter. The largest difference appeared in subzone D, probably because snow depth, biomass and vegetation height contrasts between PGF and bPG microhabitats were greatest in this subzone.

The active layer was thickest, about 90 cm, in PGFs microhabitats in subzone D, and thin (< 35 cm) in the bPGF microhabitats at both ends of the NAAT (Fig. 8c).

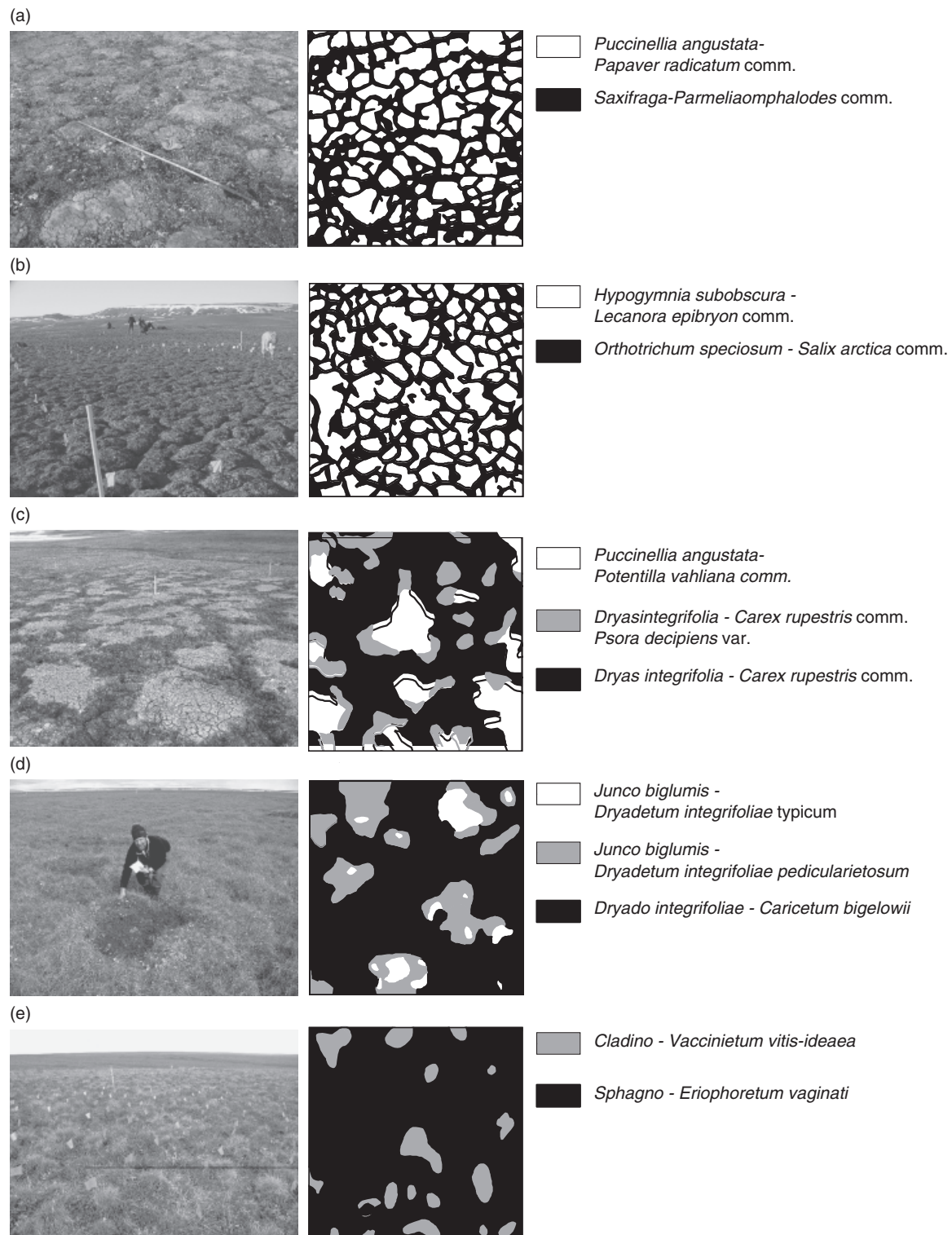


Fig. 5. Maps of plant communities in zonal patterned-ground landscapes along the NAAT. (a) Small non-sorted polygons, subzone A; (b) Small non-sorted polygons, subzone B; (c) Medium-size non-sorted circles, subzone C; (d) Medium-size non-sorted circles, subzone D; (e) Small, non-sorted circles, subzone E. Maps were standardized to display 5 × 5-m portions of the grids because only 5 × 5-m portions of the grids were mapped at Isachsen and Mould Bay; White: central patterned-ground feature (cPGF), grey: intermediate patterned-ground feature (iPGF), black: between patterned-ground feature (bPGF). Modified from Reynolds et al. (2008).

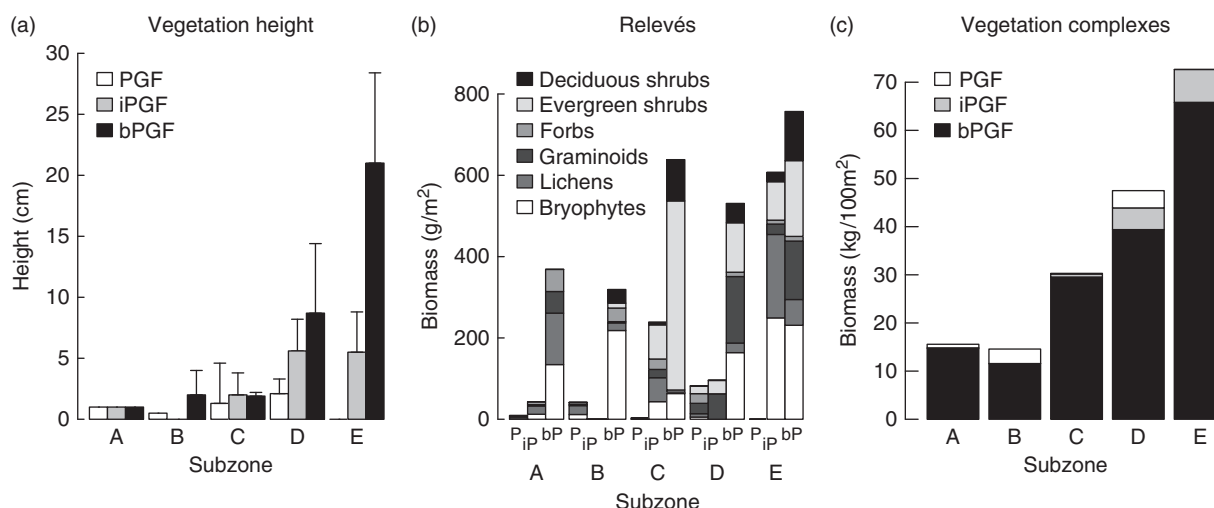


Fig. 6. Vegetation height and biomass along the NAAT. (a) Mean \pm SD of vegetation height. White: barren or sparsely vegetated centres of patterned-ground features (PGF), vegetated portions on patterned-ground features (iPGF), black: continuous vegetation between patterned-ground features (bPGF). (b) Biomass estimates for 1-m² relevés according to plant functional type. (c) Biomass estimates for 10 \times 10-m grids of vegetation complexes at Isachsen, Mould Bay, Green Cabin, Franklin Bluffs and Happy Valley.

In all cases, thaw was greater in PGFs than bPGFs, albeit measures were not adjusted for PGF height. Active layer trends corresponded well to thawing degree-days at the soil surface (Fig. 3a). Similarly, decreasing FDD measures along the transect corresponded to increasing snow depth (Fig. 3c).

Heave was most pronounced in the sparsely vegetated PGFs of subzone D, with a maximum vertical movement of 20 cm (Fig. 8d). The surrounding well-vegetated areas heaved only 2 cm. Similar low amounts of heave were found on all well-vegetated bPGF soils along the NAAT. For subzone A as well as for iPGFs in subzone E, no heave measurements were available.

Discussion

The effects of vegetation structure and composition on soil temperatures

As one moves from north to south, several factors important to colonization of PGF microhabitats change with warmer summer air temperatures. First, the suite of dominant plant growth forms that are available to colonize the PGFs changes along the bioclimate gradient. In the coldest part of the Arctic (subzone A), biological soil crusts, small lichens and bryophytes capable of colonizing the small fissures and cracks of the highly frost-active soils are the first to appear. These are followed by only a few small herbaceous species such as *Alopecurus alpinus*, *Phippsia algida*, *Luzula nivalis*, *Juncus biglumis*, *Cardamine bellidifolia*, *Cochlearia arctica*, *Papaver radicatum*, *Saxifraga cespitosa*, *S. cernua*, *S. oppositifolia*, *Draba capitata* and *Stellaria edwardsii*

s.l. The total vascular flora of subzone A consists of only about 50 species (Young 1971). There are no woody plants or sedges, which are so important for colonization further south. In the middle portion of the climate gradient (subzone C), the total flora pool is much larger (150–250 species), including such common colonizers on non-sorted circles as *Carex capillaris*, *Eriophorum angustifolium*, *Tofieldia pusilla*, *Pedicularis lanata*, *Polygonum viviparum*, *Braya glabella* ssp. *purpurascens*, *Koenigia islandica*, *Dryas integrifolia*, *Salix reticulata* and *Tephrosia atropurpurea*. In the Low Arctic (subzones D and E), larger herbaceous plants with strong rooting systems such as *Eriophorum vaginatum* and woody plants such as *Cassiope tetragona*, *Salix glauca*, *S. lanata*, *Ledum decumbens*, *Betula nana*, *Salix pulchra* and *Vaccinium vitis-idaea* are important colonizers. Dwarf shrubs become established first in the more stable soils around the margins of non-sorted circles and are then able to colonize the centres with creeping stems or ride invading bryophyte mats that are not anchored to the frost-active soils.

In summer, the most important vegetation factors affecting soil thermal regimes of patterned-ground soils are the thickness and biomass of the plant cover. In subzone E, the much greater height of the vegetation (Fig. 6a) and the presence of tussock sedges (*Eriophorum vaginatum* and *Carex bigelowii*) act to shade the soil from direct solar radiation. The larger amount of biomass on bPGF microhabitats in subzones D and E and on PGFs in subzone E (Fig. 6b) act to insulate the mineral soils and create the low summer *n*-factors observed in bPGF microhabitats of subzone D and in both PGF and bPGF microhabitats of subzone E (Fig. 8a). Thick soil organic horizons, exceeding 10 cm, in subzones D and E (Walker

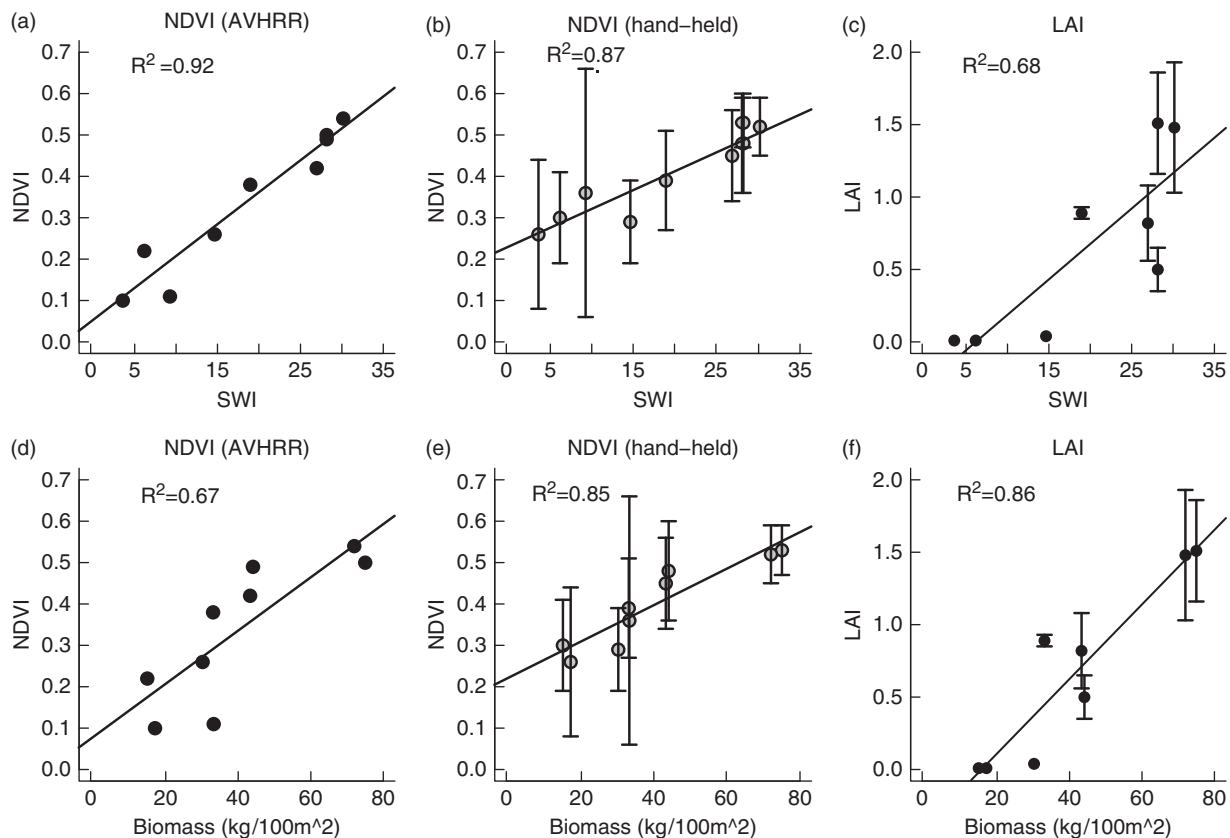


Fig. 7. NDVI and LAI versus summer warmth and biomass. (a–c) AVHRR-derived NDVI, hand-held NDVI, and LAI versus SWI. (d–f) AVHRR-derived NDVI, hand-held NDVI, and LAI versus biomass. The AVHRR values are from single AVHRR pixels at the locations of the mapped grids in each subzone. Hand-held NDVI and LAI values are from instrumental measurements along 50-m transects adjacent to the 10 × 10-m gridded landscapes in each subzone. SWI units are °C mo. Landscape-level biomass was determined by using the average biomass of vegetation types in each zonal vegetation complex (determined from clip harvests of relevé plots) and weighting these according to the area of each vegetation type in maps of the 10 × 10-m zonal grids. Error bars are standard deviations. See Methods for details.

et al. 2008a, data not shown here) also contribute to the total summer insolation above the mineral soil. In winter, the thermal contrasts between the PGF and bPGF microhabitats are much reduced. The vegetation layer has little effect on winter soil temperatures, but snow does. The deeper snow in subzones D and E acted to reduce the winter *n*-factors. The effect of microhabitat is also much reduced in winter.

The *n*-factor provides a good indication of the effects of the vegetation on the thermal properties of the soil, but it cannot be used to calculate the actual heat flux, which is necessary to develop a physically-based model of patterned-ground formation. Other investigators in biocomplexity studies estimated the mean *R*-value of the tundra organic mats. The *R*-value is a measure of thermal resistance, measured as m² K/W, which can be used to calculate the heat flux. The heat flux and *R*-values of tundra vegetation are exceptionally hard to measure, mostly due to the constantly varying amount of water in the organic layers and changes in state of the water, from

liquid to vapour or ice. Daanen et al. (2008) used the depth of snow and biomass of the measured plant growth forms at each of the NAAT relevés to develop a multiple linear regression equation to predict the *R*-value of tundra at each NAAT relevé and compared this to the *R*-values required to predict a known active layer at each relevé from a coupled heat and moisture transport model ($R^2 = 0.82$) (Daanen et al. 2008).

Nikolsky and others (2008) developed a thermo-mechanical model of frost heave based on mass, momentum and energy conservation laws for water, ice and soil, where the predictions agreed well with measured dynamics of soil temperature, water content and frost heave at one of the biocomplexity study sites (Nikolsky et al. 2008). They then examined the sensitivity of the heave model to varying thicknesses of organic layers, based on a field experiment that empirically determined the effect of removing or adding moss mats on active layer depths and soil heave (Kade & Walker 2008). They found that without a moss mat, the centres of the modelled non-sorted

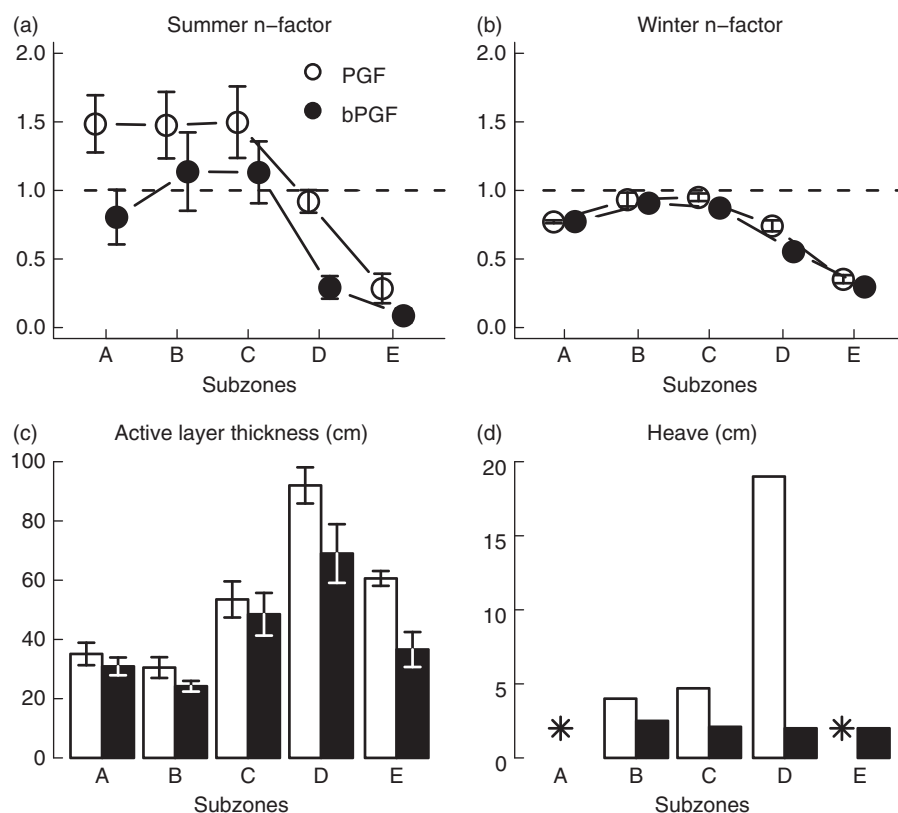


Fig. 8. Summer and winter n -factors, active layer thickness and heave along the NAAT. White: centres of patterned-ground features (PGF); black: continuous vegetation between patterned-ground features (bPGF). Error bars = standard deviation; asterisk = missing values.

circle would heave about 17 cm. Adding 2 cm of moss reduced the heave to about 12 cm and adding 10 cm of moss reduced it to about 6 cm.

For all of these modelling efforts, it was important to characterize the microhabitats, species composition and structure of the plant communities growing on the PGFs compared to the areas between the PGFs. It was also important to recognize and map the mosaic of plant communities growing on microhabitats to arrive at better biomass estimates of zonal landscapes in each subzone. Future characterization of zonal vegetation and vegetation in arctic landscapes with patterned-ground will need to weigh the benefits and time required to characterize the vegetation of each element of the patterned-ground landscape. Matveyeva (1998) recognized the small microhabitats and mapped many of them, but chose to use larger relevés for characterization of the zonal vegetation along a climate gradient on the Taimyr Peninsula. This was important to develop complete species lists for these large landscapes. However, it is not possible to determine the area and composition of the vegetation growing in the patterned-ground microhabitats from her data. We would recommend a compromise approach in these landscapes, where larger plots that encompass the full suite of

microhabitats on patterned-ground are used, but that a small sketch map be made of the plot showing the various microhabitats, with their estimated areas, and that the cover-abundance of each species be estimated for the whole plot as well as the microhabitats within the plot.

Summary of interactions between vegetation and patterned-ground features along the Arctic bioclimate gradient

We use a modification of the Matveyeva's and Shur's conceptions of changes along primary succession sequences to illustrate the typical patterns of patterned-ground and vegetation along the NAAT (Fig. 9). We incorporate new information from our transect and include reference to physical processes of patterned-ground formation in relation to permafrost, thermal and hydrological conditions within the PGFs (Peterson & Krantz 2003; Shur et al. 2005, 2008; Daanen et al. 2008; Nikolsky et al. 2008).

In the colder parts of the Arctic, in bioclimate subzones A, B and C, small non-sorted polygons about 10–30 cm in diameter (Figs 1a,b and 9 stage a) occur abundantly on most surfaces. The origin of the cracks between these polygons has been disputed and is thought to be due to either desiccation cracking or thermal contraction

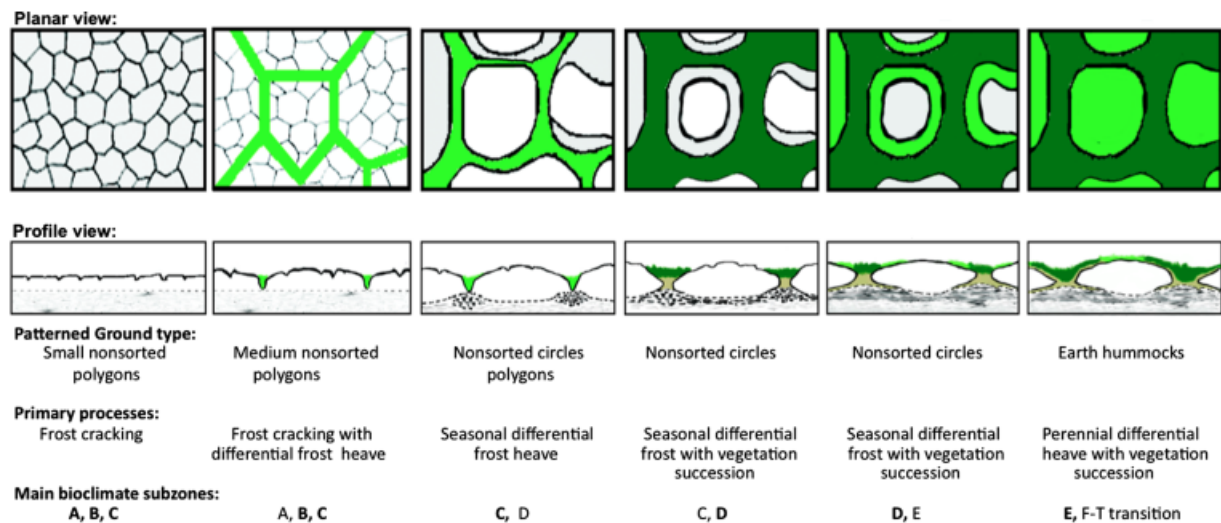


Fig. 9. Conceptual sequence of patterned-ground features along the Arctic bioclimate gradient. (a) Small non-sorted polygons 20–30 cm in diameter that are barren or with biological soil crust vegetation. (b) Differential frost heave causes the formation of intermediate-scale polygons 1–2 m in diameter with colonization by small forbs, bryophytes and lichens in the cracks of the larger polygons. (c) Formation of non-sorted circles. Deepening and widening of the secondary cracks with additional vegetation, which reduces the heat flux and active layer thickness (dashed lines in profile views) in the areas between the circles and enhances differential frost heave. Differential heave is annual, with mound development in winter and collapse during the summer. (d) Colonization of the non-sorted circles, first by small cryptogamic species and small forbs, and (e) more actively by thicker moss mats and more diverse plant communities. Initiation of perennial mound formation is due to strong differential frost heave and an aggrading permafrost table. (f) Earth hummocks formed by complete colonization of the hummock surface by a thick vegetation mat. The mound develops as permafrost aggrades in the bowl-shaped depressions in the permafrost table beneath the mounds, causing perennial differential frost heave. The bolded subzones listed as 'Main bioclimate subzones' are where the forms are maximally expressed. The model expands on Matveyeva's concept for the planar views and Shur's concept for the profile views (Chernov & Matveyeva 1997; Shur et al. 2008).

cracking or a combination of the two. Our studies indicate that thermal contraction cracking is the likely primary cause for most of the small polygons because they are ubiquitous on nearly all hill slope positions in bioclimate subzones A, B and C, even moderately steep slopes and very humid areas of these subzones, such as Franz Josef Land in Russia, where they form in soils of all textures including sands; whereas desiccation polygons usually form on soils with considerable clay content and on flat areas and depressions where water tends to pool.

In the coldest areas of subzone A, the tops of the small polygons are often not vegetated or covered with biotic soil crusts, but the cracks between these polygons are favourable microhabitats for colonization by bryophytes, lichens and small herbaceous plants. In some areas of subzone A and in subzones B and C, the small polygons are more vegetated and rounded into small hummocks (Fig. 1b).

Medium-size, non-sorted polygons (50–200 cm diameter) can occur in loamy soils of subzone A, but are more common in subzones B and C, and are also common but less apparent in subzones D and E, where they are often masked by vegetation (Figs 1c and 9 stage b).

What causes the intermediate-size polygons? Our observations suggest that differential frost heave acts to

group the small polygons into medium-size, non-sorted polygons. At our Howe Island study location, we found an area of polygons that has been periodically inundated during storm surges with salt water that killed much of the vegetation and exposed details of the underlying patterned-ground (Fig. 10). Polygonal patterns occurred at three primary scales: (1) small polygons approximately 20–30 cm in diameter most likely caused by shallow frost cracking (Fig. 10a); (2) medium-size polygons, approximately 2–3 m in diameter that contain a non-sorted circle in the centre of each polygon (Fig. 10a, b); and (3) approximately 10–20 m large polygons associated with large ice wedges (Fig. 10c). The pattern of medium-size polygons and non-sorted circles suggests that heaving associated with non-sorted circles is responsible for organizing the smaller polygons into larger groups and that vegetation most actively colonizes the cracks between the medium-size polygons. The lower topographic positions in the cracks have more protected and stable soils and enhanced water and nutrient availability, which promote plant growth.

Most non-sorted circles that we observed were associated with medium-size polygons at 2–3-m scale, and often there are well developed cracks around the margins of the polygons; however, in rocky soils or in heavily

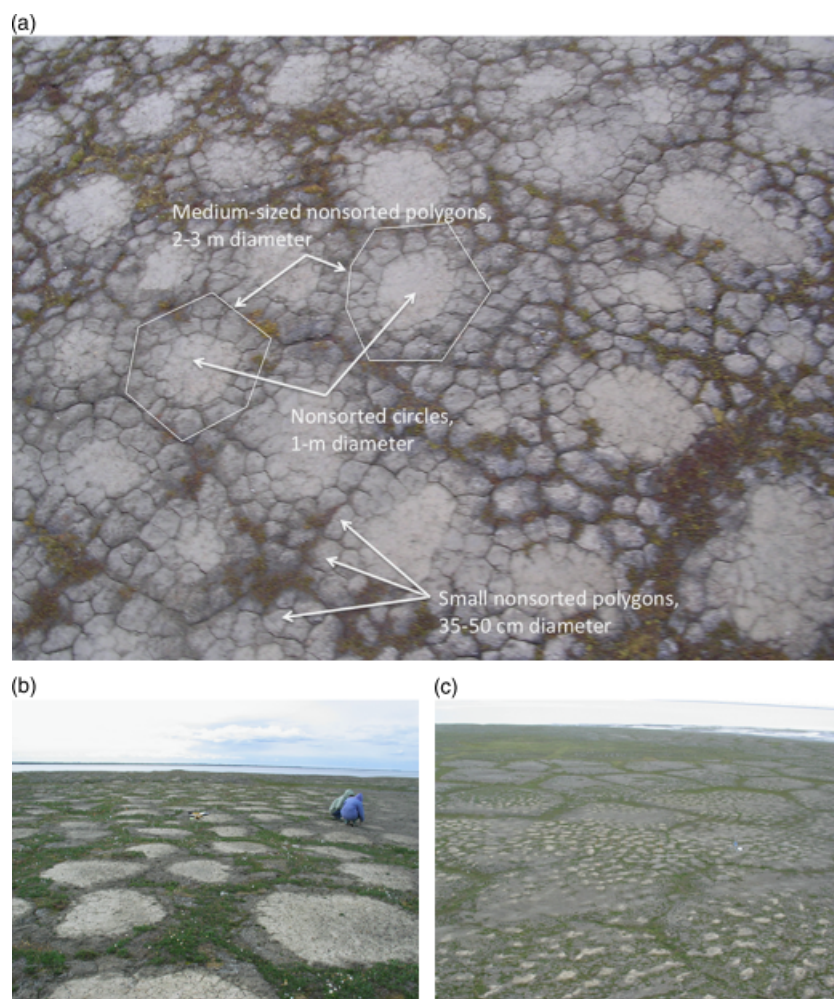


Fig. 10. Patterns of polygons and circles on Howe Island, AK. This location is periodically inundated with salt water during storm surges, which kills much of the vegetation and exposes details of the underlying patterned ground that probably initially formed when the island was part of the mainland and more distant from the coast. **(a)** Vertical view showing a complex of small, non-sorted polygons (20–30-cm diameter), non-sorted circles (90–200-cm diameter), and medium-size polygons (200–300-cm diameter). **(b)** Ground view of non-sorted circles. The centres of the circles are nearly barren; the grey margins are small non-sorted polygons with lichens and biological soil crusts; and the green areas are dominated by *Dryas integrifolia* and *Salix ovalifolia*. **(c)** Ice wedge polygons with diameters of 10–30 m. Ice wedges, which form by deep thermal cracking into the permafrost, are located beneath the green borders of the polygons. Numerous non-sorted circles occur in the centres of the large polygons.

vegetated areas, the cracks or the non-sorted circles, or both, are often masked. During our investigations of non-sorted circle formation, we focused on the process of differential heave. The phenomenon of cracking was not modelled during the project because we did not initially realize the strong interrelationship between the scale of frost heave and the scale of cracking.

There is currently no proven method in which differential frost heave can occur in the absence of differential surface temperatures, such as that associated with heterogeneously vegetated surfaces; however, a model developed by Peterson & Krantz (2003) does advance a theory that involves linear stability theory and nonlinear numerical analysis to explain how a pattern of non-sorted circles can

be initiated in the absence of a vegetative cover, which may help explain the spacing of non-sorted circles and the crack spacing of the intermediate-scale polygons.

Once the pattern is established, the depressions in the cracks between the heave features are topographic low points. These protected sites also collect water and nutrients and enhance plant growth. The accumulation of vegetation in the cracks and the products of decomposition change the thermal properties of the active layer in the vicinity of the cracks, as evidenced from the *n*-factor trends and active-layer data (Fig. 8a-c). The soil temperature differential between the centres and margins of the polygons, caused by the presence of the vegetation, enhances differential frost heave and initiates the

formation of bowl-shaped depressions in the permafrost beneath the polygons (Shur et al. 2008). These bowl-shaped depressions are interpreted from the thaw-layer thickness data, which show maximum thaw-layer thickness in the centres of the polygons and less in the cracks between polygons (Fig. 8c, dashed line). The change in morphology of the permafrost table is important because it controls the subsurface flow and pooling of water and organic matter, which collect in the basins beneath the polygons and further affect the heat differentials within the polygons (Shur et al. 2008).

In subzones C and D, non-sorted circles are a prominent component of most zonal landscapes (Figs 1c, d and 9 stages c, d). Thick active layers occur in the barren mineral soils in the centres of the circles, and thinner active layers occur where organic material forms and accumulates in the bPFGF areas. More robust vegetation, with considerable biomass and organic soil horizons, develops in the troughs associated with the contraction cracks. This is the stage of greatest thermal contrast between the PFGF and bPFGF microhabitats and the stage of maximum *seasonal* differential frost heave. Seasonal heave is the result of small ice lenses that form each winter within the annually frozen soils, causing the soils to heave, and which melt every summer causing the soils to collapse. Heave in the areas between the PGFs is minimal because of the thick organic layers. As a consequence, non-sorted circle morphology is best developed at this stage with relatively barren frost-active centres and well-vegetated bPFGF areas.

Further south, in the warmer climates of bioclimate subzones D and E, vegetation actively colonizes the margins of the circles and spreads over the active centres (Fig. 9 stage d, e). This begins stabilization of the surface and reduces the summer heat flux in the centres of the features. This reduces thickness of the active layer in the centres of the polygons, but differential heave is maintained through the summer. Eventually, this process leads to the formation of *earth hummocks* (Figs 1e, f and 9 stage e). Shur et al. (2005, 2008) show that as the vegetation and soil organic matter build in the centres of the non-sorted circles, the active layer is reduced in thickness, and aggradational ice (new ice added to the top of the permafrost table) develops beneath the polygons. This causes the centres of the circles to become permanently elevated relative to the troughs over the cracks, forming the earth mounds. The *perennial differential frost heave* associated with earth mounds is distinct from the *annual differential frost heave* that occurs with most non-sorted circles. Perennial frost heave is the result of a slowly aggrading permafrost table. The process is more thoroughly explained in a conceptual model presented by Shur et al. (2008). Most earth mounds that we observed

were in well-vegetated areas of subzone E and the boreal forest.

A retrogressive phase of earth mound development can occur when the vegetation mat on the mound is destroyed by fire or other disturbances (Kokelj et al. 2007; Shur et al. 2008). This leads to thawing of the aggradational ice and to substantial thaw settlement and even total collapse of the mound. If conditions permit, the process of vegetation succession and building of the aggradational ice will repeat and rebuild the mound.

Acknowledgements

D.A. Walker and P.J. Kuss are the principal authors and contributed equally to this paper. The other authors made important major contributions to the content. We thank Olga Afonina, Aleksei Potemkin and Mikhael Zhurbenko for identification of bryophytes and lichens; Chien-Lu Ping and Gary Michaelson for soil chemical and physical analysis; Vladimir Romanovsky for climate and frost heave data; Corinne Munger for plant community maps; Jamie Hollingsworth, Lindsey Kiesz, Julie Knudson, Katie Mohrmann, Miriah Phelps, Galina Popova and Daniel Walker for assistance in the field and biomass laboratory; Ronnie Daanen, William Gould, Grizelle Gonzalez, Alexia Kelley, William Krantz, Nadya Matveyeva, Gosha Matyshak, Rorik Peterson, Yuri Shur, Charles Tamocai and Ina Timling for conceptual discussions; and Milan Chytrý for producing the synoptic table in JUICE. We further thank VECO Polar Resources and Aklak Air for logistical support, and Parks Canada and the Inuvialuit community for supporting our study on their lands. The authors also acknowledge the generous support of US National Science Foundation grants OPP-0120736, ARC-0425517 to DAW, a German Research Foundation grant to FJAD, a Swiss National Science Foundation grant PBBE2-108513 to CV, and NASA grants NNG6GE00A and NNX09AK56G for support in preparation of this synthesis.

References

- Alexandrova, V.D. 1980. *The Arctic and Antarctic: their division into geobotanical areas*. Cambridge University Press, Cambridge, UK.
- Brown, J., Hinkel, K.M. & Nelson, F.E. 2000. The circumpolar active layer monitoring (CALM) program: research designs and initial results. *Polar Geography* 24: 165–258.
- Carlson, H. 1952. Calculation of depth of thaw in frozen ground. Highway Research Board Special Report 2, National Research Council, Washington, DC.
- CAVM Team. (Gold, W.A., Bliss, L.C., Edlund, S.A., Reynolds, M.K., Zoltai, S.C., Daniëls, F.J.A., Bay, C., Wilhelm, M., Einarsson, E., Gundjónsson, Elvebakk, A. Johansen, B.E. Ananjeva, G.V.,

- Drozdo, D.S., Katenin, A.E., Kholod, S.S., Konchenko, L.A., Korostelev, Y.V., Melnikov, E.S., Moskolenko, N.G., Polekhaev, A.N., Ponomareva, O.E., Pospelova, E.B., Safronova, I.N., Shelkunova, R.P., Yurtsev, B.A., Fleming, M.D., Markon, C.J., Murray, D.F., Talbot, S.S., Walker, D.A. 2003. *Circumpolar Arctic vegetation map*. Conservation of Arctic Flora and Fauna (CAFF) Map No. 1, US Fish and Wildlife Service, Anchorage, AK.
- Chernov, Y.I. & Matveyeva, N.V. 1997. Arctic ecosystems in Russia. In: Wielgolaski, F.E. (ed.) *Polar and alpine tundra*. Vol. 3, pp. 361–507. Elsevier, Amsterdam, NL.
- Daanen, R.P., Misra, D., Epstein, H., Walker, D. & Romanovsky, V. 2008. Simulating nonsorted circle development in arctic tundra ecosystems. *Journal of Geophysical Research – Biogeosciences* 113: 1–10.
- Daniëls, F.J.A., Elvebakk, A., Talbot, S.S. & Walker, D.A. (eds.) 2005. Classification and mapping of arctic vegetation: A tribute to Boris A. Yurtsev. *Phytocoenologia* 35: 715–1079, Special issue.
- Elven, R., Murray, D.F., Razzhivin, D.F. & Yurtsev, B.A. 2007. *Checklist of the Panarctic Flora (PAF) vascular plants*. Draft. University of Oslo, Oslo, NO.
- Epstein, H.E., Gould, W.A., Kelley, A.M., Kade, A.N., Knudson, J.A., Krantz, W.B., Michaleson, G., Peterson, R.A., Ping, C.L., Reynolds, M.K., Romanovsky, V.E. & Shur, Y.L. 2004. Frost-boil ecosystems: complex interactions between landforms, soils, vegetation, and climate. *Permafrost and Periglacial Processes* 15: 171–188.
- Epstein, H.E., Walker, D.A., Reynolds, M.K., Jia, G.J. & Kelley, A.M. 2008. Phytomass patterns across a temperature gradient of the North American arctic tundra. *Journal of Geophysical Research – Biogeosciences* 113: 1–11.
- Esslinger, T.L. 2008. A cumulative checklist for the lichen-forming, lichenicolous and allied fungi of the continental United States and Canada Version #14. Available at: <http://www.ndsu.nodak.edu/instruct/esslinge/chcklst/chcklst7.htm>. First posted 1 December 1997. North Dakota State University, Fargo, ND.
- Everett, K.R. 1968. *Soil development in the Mould Bay and Isachsen areas, Queen Elizabeth Islands, Northwest Territories, Canada*. Report no. 24, Institute of Polar Studies, Ohio State University, Columbus, OH.
- Everett, K.R. & Parkinson, R.J. 1977. Soil and landform associations, Prudhoe Bay area, Alaska. *Arctic and Alpine Research* 9: 1–19.
- Hallet, B. 1987. On geomorphic patterns with a focus on stone circles viewed as a free-convection phenomenon. In: Nicolis, C. & Nicolis, G. (eds.) *Irreversible phenomenon and dynamical systems analysis in geosciences*. pp. 533–553. Reidel Publishing, Dordrecht, NL.
- Hamilton, T.D. 1986. Late Cenozoic glaciation of the Central Brooks Range. In: Hamilton, T.D., Reed, K.M. & Thorson, R.M. (eds.) *Glaciation in Alaska: the geologic record*. pp. 9–48. Alaska Geological Society, Anchorage, AK, US.
- Hennekens, S.M. & Schaminée, J.H.J. 2001. TURBOVEG, a comprehensive data base management system for vegetation data. *Journal of Vegetation Science* 12: 589–591.
- Heywood, W.W. 1957. Isachsen area, Ellef Ringnes Island district of Franklin Northwest Territories. Paper 56–8, Geological Survey of Canada, Ottawa, CA.
- Hopkins, D.M. & Sigafos, R.A. 1951. Frost action and vegetation patterns on Seward Peninsula, Alaska. Report no. 974-C, US Geological Survey, Washington, DC, US.
- Ignatov, M.S. & Afonina, O.M. 1992. Check-list of mosses of the former USSR. *Arctoa* 1: 1–86.
- Kade, A. & Walker, D.A. 2008. Experimental alteration of vegetation on nonsorted circles: effects on cryogenic activity and implications for climate change in the Arctic. *Arctic, Antarctic and Alpine Research* 40: 96–103.
- Kade, A., Walker, D.A. & Reynolds, M.K. 2005. Plant communities and soils in cryoturbated tundra along a bioclimate gradient in the Low Arctic, Alaska. *Phytocoenologia* 35: 761–820.
- Kade, A., Romanovsky, V.E. & Walker, D.A. 2006. The N-factor of nonsorted circles along a climate gradient in Arctic Alaska. *Permafrost and Periglacial Processes* 17: 279–289.
- Karunaratne, K.C. & Burn, C.R. 2003. Freezing n-factors in discontinuous permafrost terrain, Takhini River, Yukon Territory, Canada. In: Phillips, M., Springman, S.M. & Arenson, L.U. (eds.) *Permafrost: Proceedings of the Eighth International Conference on Permafrost*. pp. 519–524. A.A. Balkema, Zurich, CH.
- Kessler, M.A. & Werner, B.T. 2003. Self-organization of sorted patterned-ground. *Science* 299: 380–383.
- Klene, A.E., Nelson, F.E. & Shiklomanov, N.I. 2001a. The n-factor as a tool in geocryological mapping seasonal thaw in the Kuparuk River Basin, Alaska. *Physical Geography* 22: 449–466.
- Klene, A.E., Nelson, F.E., Shiklomanov, N.I. & Hinkel, K.M. 2001b. The n-factor in natural landscapes: variability of air and soil-surface temperatures, Kuparuk River Basin, Alaska U.S.A. *Arctic, Antarctic and Alpine Research* 33: 140–148.
- Kokelj, S.V., Burn, C.R. & Tarnocai, C. 2007. The structure and dynamics of earth hummocks in the subarctic forest near Inuvik, Northwest Territories, Canada. *Arctic, Antarctic and Alpine Research* 39: 99–109.
- Konstantinova, N.A., Potemkin, A.D. & Schljakov, R.N. 1992. Checklist of the Hepaticae and Anthocerotae of the former USSR. *Arctoa* 1: 87–127.
- Kristinsson, H., Zhurbenko, M.P. & Hansen, E.S. 2010. Panarctic checklist of lichens and lichenicolous fungi. Report no. 20, CAFF International Secretariat, Akureyri, IS.
- Matveyeva, N.V. 1994. Floristic classification and ecology of tundra vegetation of the Taymyr Peninsula, northern Siberia. *Journal of Vegetation Science* 5: 813–828.
- Matveyeva, N.V. 1998. *Zonation of plant cover in the Arctic*. Russian Academy of Science, St. Petersburg, RU [In Russian].
- McCune, B., Grace, J.B. & Urban, D.L. 2002. *Analysis of ecological communities*. MjM Software Design, Gleneden Beach, OR, US.
- Michaelson, G.L., Ping, C.L., Epstein, H.E., Kimble, J.M. & Walker, D.A. 2008. Soils and frost boil ecosystems across

- the North American Arctic Transect. *Journal of Geophysical Research - Biogeosciences* 113: G03S11.
- Nelson, F., Brown, J., Lewkowicz, T. & Taylor, A. 1996. Active layer protocol. In: Molau, U. & Molgaard, P. (eds.) *ITEX manual*. 2nd ed, pp. 14–16. International Tundra Experiment, Copenhagen, DK.
- Nicholson, F.H. 1976. Patterned ground formation and description as suggested by low arctic and subarctic examples. *Arctic and Alpine Research* 8: 329–342.
- Nikolsky, D.J., Romanovsky, V.E., Tipenko, G.S. & Walker, D.A. 2008. Modeling biogeophysical interactions in non-sorted circles in the Low Arctic. *Journal of Geophysical Research - Biogeosciences* 113: G03S04.
- Osterkamp, T.E. 2003. Establishing long-term permafrost observations for active-layer and permafrost investigations in Alaska: 1977–2002. *Permafrost and Periglacial Processes* 14: 331–342.
- Peterson, R.A. & Krantz, W.B. 2003. A mechanism for differential frost heave and its implications for patterned-ground formation. *Journal of Glaciology* 49: 69–80.
- Ping, C.L., Michaelson, G.J., Kimble, J.M., Romanovsky, V.E., Shur, Y.L., Swanson, D.K. & Walker, D.A. 2008. Cryogenesis and soil formation along a bioclimate gradient in Arctic North America. *Journal of Geophysical Research - Biogeosciences* 113: G03S12.
- Raynolds, M.K., Walker, D.A., Munger, C.A., Vonlanthen, C.M. & Kade, A.N. 2008. A map analysis of patterned-ground along a North American Arctic Transect. *Journal of Geophysical Research - Biogeosciences* 113: G03S03.
- Razzhivin, V.Y. 1999. Zonation of vegetation in the Russian Arctic. In: Nordal, I. & Razzhivin, V.Y. (eds.) *The species concept in the high north - A panarctic flora initiative*. pp. 113–130. The Norwegian Academy of Science and Letters, Oslo, NO.
- Romanovsky, V.E., Marchenko, S.S., Daanen, R., Sergeev, D.O. & Walker, D.A. 2008. Soil climate and frost heave along the permafrost/ecological North American Arctic transect. In: Kane, D.I. & Hinkel, K.M. eds. *Proceedings Ninth International Conference on Permafrost*. pp. 1519–1524. Institute of Northern Engineering, University of Alaska, Fairbanks, AK, US.
- Shur, Y., Ping, C.L. & Walker, D.A. 2005. Comprehensive model of frost boils and earth hummock formation. 2nd European Conference on Permafrost. Terra Nostra, Potsdam, DE. p. 79.
- Shur, Y., Jorgenson, T., Kanevskiy, M. & Ping, C.-L. 2008. Formation of frost boils and earth hummocks. In: Kane, D.I. & Hinkel, K.M. eds. *Ninth International Conference on Permafrost, extended abstracts*. pp. 287–288. Institute of Northern Engineering, University of Alaska, Fairbanks, AK, US.
- Stott, D.F. 1969. Ellef Ringnes Island, Canadian Arctic Archipelago. Report no. 68-16, Geological Survey of Canada, Department of Mines and Resources, Ottawa, CN.
- Stow, D.A., Hope, A., D., M., Verbyla, D., Gamon, J., Huemmerich, F., Houston, S., Racine, C., Sturm, M., Tape, K., Hinzman, L., Yoshikawa, K., Tweedie, C., Noyle, B., Silapaswan, C., Douglas, D., Griffith, B., Jia, G., Epstein, H., Walker, D., Daeschner, S., Petersen, A., Zhou, L. & Myneni, R. 2004. Remote sensing of vegetation and land-cover change in arctic tundra ecosystems. *Remote Sensing of Environment* 89: 281–308.
- Taylor, A.E. 2001. Relationship of ground temperature to air temperatures in forests. In: Dyke, L.D. & Brookes, G.R. eds. *The physical environment of the Mackenzie Valley: A baseline for the assessment of environmental change*. Vol. 547, pp. 111–117. Geological Survey of Canada Bulletin, Ottawa, CA.
- Tedrow, J.C.F., Bruggemann, P.F. & Walton, G.F. 1968. Soils of Prince Patrick Island. Report no. 44, Office of Naval Research, Washington, DC, US.
- Tichý, L. 2002. JUICE, software for vegetation classification. *Journal of Vegetation Science* 13: 451–443.
- Tichý, L. & Chytrý, M. 2006. Statistical determination of diagnostic species for site groups of unequal size. *Journal of Vegetation Science* 17: 809–818.
- Tucker, C.J. & Sellers, P.J. 1986. Satellite remote sensing of primary production. *International Journal of Remote Sensing* 7: 1395–1416.
- USDA. 1996. Soil survey laboratory methods manual. Report No. 42, Version 3.0, Natural Resources Conservation Service, National Soil Survey Center, US Department of Agriculture, Washington, DC, US.
- van Everdingen, R.O. 1998. *Multi-language glossary of permafrost and related ground-ice terms*. University of Calgary, Calgary, AB, CA.
- Vincent, J.-S. 1982. The quaternary history of Banks Island, N.W.T., Canada. *Geographie Physique et Quaternaire* 36: 209–232.
- Vincent, J.-S. 1990. Late Tertiary and early Pleistocene deposits and history of Banks Island, southwestern Canadian Archipelago. *Arctic* 43: 339–363.
- Vonlanthen, C.M., Walker, D.A., Raynolds, M.K., Kade, A., Kuss, H.P., Daniëls, F.J.A. & Matveyeva, N.V. 2008. Patterned-ground plant communities along a bioclimate gradient in the High Arctic, Canada. *Phytocoenologia* 38: 23–63.
- Vysotsky, G.N. 1909. On phyto-topological maps, approaches to compilation of them and their practical significance. *Pochvovedenie* 2: 97–124 [In Russian].
- Walker, M.D., Daniëls, F.J.A. & van der Maarel, E. 1994a. Circumpolar arctic vegetation: introduction and perspectives. *Journal of Vegetation Science* 5: 757–764.
- Walker, M.D., Walker, D.A. & Auerbach, N.A. 1994b. Plant communities of a tussock tundra landscape in the Brooks Range Foothills, Alaska. *Journal of Vegetation Science* 5: 843–866.
- Walker, D.A., Raynolds, M.K., Daniëls, F.J.A., Einarsson, E., Elvebakk, A., Gould, W.A., Katenin, A.E., Kholod, S.S., Markon, C.J., Melnikov, E.S., N.G., M., Talbot, S.S. & Yurtsev, B.A. & CAVM Team 2005. The circumpolar arctic vegetation map. *Journal of Vegetation Science* 16: 267–282.
- Walker, D.A., Epstein, H.E., Romanovsky, V.E., Ping, C.L., Michaelson, G.J., Daanen, R.P., Shur, Y., Peterson, R.A.,

- Krantz, W.B., Raynolds, M.K., Gould, W.A., Gonzalez, G., Nicolsky, D.J., Vonlanthen, C.M., Kade, A.N., Kuss, P., Kelley, A.M., Munger, C.A., Tarnocai, C.T., Matveyeva, N.V. & Daniëls, F.J.A. 2008a. Arctic patterned-ground ecosystems: a synthesis of field studies and models along a North American Arctic Transect. *Journal of Geophysical Research* 113: G03S01.
- Walker, D.A., Epstein, H.E. & Welker, J.M. (eds.) 2008b. Biocomplexity of Arctic Tundra ecosystems. *Journal of Geophysical Research* 113: G03S01-12. 147pp, Special Section.
- Walker, D.A., Orekhov, P., Frost, G.V., Matyshak, G., Epstein, H.E., Leibman, M.O., Khitun, O., Khomotov, A., Daanen, R., Gobroski, K. & Maier, H.A. 2009. The 2009 Yamal Expedition to Ostrov Belyy and Kharp, Yamal Region, Russia. Data Report, Alaska Geobotany Center, Fairbanks, AK, US.
- Washburn, A.L. 1980. *Geocryology: a survey of periglacial processes and environments*. Halsted Press, John Wiley and Sons, New York, NY, US.
- Westhoff, V. & Van der Maarel, E. 1973. The Braun-Blanquet approach. In: Whittaker, R.H. (ed.) *Ordination and classification of communities*. pp. 617–726. Dr. W. Junk, Den Haag, NL.
- Young, S.B. 1971. The vascular flora of St. Lawrence Island with special reference to floristic zonation in the arctic regions. *Contributions from the Gray Herbarium* 201: 11–115.
- Yurtsev, B.A. 1994. The floristic division of the Arctic. *Journal of Vegetation Science* 5: 765–776.
- Appendix S2.** Raw species data for the 147 relevés used in the analyses. Braun-Blanquet cover-abundance scores were transformed to percentages: r = 1, + = 2, 1 = 3, 2 = 13, 3 = 38, 4 = 68, 5 = 88.
- Appendix S3a.** Environmental and soils data legend. Explanation of categories in header of Appendix S3b.
- Appendix S3b.** Environmental and soils data for all relevés used in the analysis. Header provides labels for columns. Explanation of categories and units for each category are in Appendix S3a.
- Appendix S4.** Biomass (g m^{-2}) according to sorted categories for each relevé included in the analysis. BM = Biomass, De. = Deciduous shrub, Ev. = Evergreen shrub, Gr. = Graminoid, Forbs = Forbs, Horstail = Horsetails, Lichens = Lichens, Mosses = Bryophytes (including liverworts), Algae = Algae, lvs = leaves, fl.fr = flowers & reproductive parts, stem = stem and woody tissues, l = live, d = attached dead, NA = No data. Relevés are ordered alphabetically according to location: DH = Deadhorse, FB = Franklin Bluffs, GC = Green Cabin, HV = Happy Valley, IA = Isachsen, MB = Mould Bay, SA = Sagwon acidic, SN = Sagwon non-acidic, WD = West Dock.
- Appendix S5.** Mean soil texture of study sites within the five bioclimate subzones (A-E) along the NAAT. White: central patterned-ground feature (PGF), black: between patterned-ground feature (bPGF).

Supporting Information

Additional Supporting Information may be found in the online version of this article:

Appendix S1. Summary of plant communities and relevés in each zonal plant community complex of the synoptic table.

Please note: Wiley-Blackwell is not responsible for the content or functionality of any supporting materials supplied by the authors. Any queries (other than missing material) should be directed to the corresponding author for the article.